J. C. Trinkle
Department of Systems and Industrial Engineering
University of Arizona
Tucson, Arizona 85721

R. P. Paul
Department of Computer and Information Science
GRASP Laboratory
University of Pennsylvania
Philadelphia, Pennsylvania 19104

Planning for Dexterous Manipulation with Sliding Contacts

Abstract

Dexterous manipulation refers to the skillful execution of object reorienting and repositioning maneuvers, especially when performed within the grasp of an articulated mechanical hand. In this paper we study the problem of gaining a secure and enveloping grasp of a two-dimensional object by exploiting sliding at the contacts between the object and the hand. This is done in two steps: first, choosing an initial grasp with which the object can be manipulated away from the support, and second, continuously altering the grasp so that envelopment is achieved. The plans generated by our technique could be executed with only position control. However, it would be prudent to incorporate contact force sensing to prevent damage during unexpected events.

The main contributions of this paper are the derivation of liftability regions *of a planar object for use in manipulation planning; the use of the* lifting phase plane *in manipulation planning; and the derivation of the quasi-static* forward object motion problem, *which provides a basis for general three-dimensional manipulation planning with rolling and/or sliding contacts.*

1. Introduction

One desirable application of robotic technology is automatic assembly using articulated mechanical hands and flexible fixturing systems. Assuming that the parts of the product to be assembled are within reach of the robot and the sequence of assembly operations is known, the following fundamental problems must be addressed: (1) part acquisition, by which is meant the synthesis and achievement of the desired grasp; (2) fixture set-up, which is closely related to grasp synthesis but additionally requires the design of an accessible partial fixture (Asada and By 1984) as an intermediate step; and (3) parts mating, which requires path planning (Brooks 1983) and compliant motion control (Mason 1979; Whitney 1982; Mason and Salisbury 1985).

Part acquisition includes the achievement of the desired grasp, which if not initially accessible, will require dexterous manipulation actions to be performed. We define dexterous manipulation as the controlled movement of the grasped part relative to the hand. In this paper, we concentrate on part acquisition via dexterous manipulation, especially for the case of frictionless objects. In so doing, we define the *liftability regions* that provide a sound means to synthesize a suitable initial grasp of an object resting on a support and a geometric method for planning subsequent dexterous manipulations. Contact forces are not controlled; they are rendered insignificant by the geometry of the grasp. Therefore manipulation can proceed under position control. However, contact force sensing (as opposed to contact force servoing) could be useful to detect jamming and to prevent damaging fragile parts.

1.1. Grasp Synthesis

Techniques for synthesizing stable grasps for articulated mechanical hands have been developed based on

The International Journal of Robotics Research,
Vol. 9, No. 3, June 1990,

quasi-static analysis coupled with optimization methods (Jameson 1985), independent regions of stable contact (Paul 1972; Nguyen 1986), expected task forces and fine motion requirements (Kobayashi 1984; Li and Sastry 1987), the forces required to cause one or more contacts to slip (Cutkosky 1985; Holzmann and McCarthy 1985), minimization of the contact forces arising from external forces (Trinkle 1985), and the potential energy in compliant fingers (Hanafusa and Asada 1982). If obstacles such as the part's supporting surface do not interfere with placing the fingers in their designated grasping configurations, then the synthesized grasp may be executed (i.e., the part is acquired). If on the other hand, one is not so lucky, then grasp acquisition must be achieved through dexterous manipulation beginning with an accessible but suboptimal grasp. This suboptimal grasp could be synthesized by adding accessibility constraints to most any grasp synthesis technique [as was done by Laugier and Pertin (1983) and Wolter et al. (1984) for the case of parallel-jawed grippers].

2. Manipulation

Most researchers considering dexterous manipulation begin their analysis from the point of an acquired grasp. For example, Okada (1982) controlled a hand to turn a nut onto a bolt, Kobayashi's (1984) experimental hand drew simple figures with a pencil, and Kerr (1984) developed the general differential equations for dexterous manipulation. These studies were done assuming only rolling contacts exist. Enforcing this assumption requires that manipulation be carried out under force and position control and unduly limits the manipulation that can be performed.

Attempts to quantify the effects of sliding during manipulation were first made by Mason and Salisbury (1985) for the case of pushed objects sliding quasi-statically in a horizontal plane. Peshkin and Sanderson (1988) found quantitative bounds on several of Mason's qualitative results by considering all possible supporting contact distributions. Also working in the plane, Brost (1985) and Erdmann and Mason (1986) developed techniques to remove all uncertainty in the orientation of planar objects, the former through squeeze grasping operations with a parallel-jawed gripper and the latter by planning a sequence of tilting operations of a rectangular tray containing the object. Another planar manipulation problem was studied by Fearing (1986; 1987), who developed a manipulation algorithm (utilizing both sliding and rolling contact states) to enable the Salisbury hand to "twirl a baton" in a vertical plane. Also using the Salisbury hand, Brock (1988) demonstrated manipulation with "controlled slip." For manipulation of a three-fingertip grasp, his method can be viewed as choosing two fingertip contacts to define an axis of rotation. Those two fingers apply a somewhat larger normal force than the third fingertip, which is dragged across the object so that its friction force applies a moment and induces rotation about the axis defined by the two fingertips. One other study on contact slippage was undertaken by Nguyen (1986). He was concerned with the stability of static grasps for which manipulation occurred "passively" (that is, the object's motion resulted from the deformation of the hand in response to changes in the external wrench applied to the object). Active manipulation was not considered.

The only work on active sliding manipulation for general three-dimensional objects has been done by Ji (1987) and Trinkle (1987). Ji's dissertation contains results for fingertip grasps analogous to those developed by Kerr (1984) for fingertips with rolling contacts. His result's major weakness is that it relies on the contacts' constraining the object such that there is a unique kinematically admissible motion. Trinkle developed the frictionless *object motion problem* specifically to predict the motion of the grasped object in response to the motion of the robot when there is more than one (usually an infinite set of) kinematically admissible motion.

In the following analysis, we consider the quasi-static motion of a manipulated object. Even though uncertainty exists in the precise descriptions of the contact forces, the resultant force and the object's geometry are always known. These facts allow exact computation of the object's instantaneous velocity given the instantaneous velocity of the palm and fingers.

Fig. 1. Two-point initial grasp.

2. Liftability of Rigid Bodies

One reason to grasp an object is to gain complete control over its position and orientation. Thus we propose that an object is grasped by a robot if the object contacts only the robot's hand. If other bodies such as the support are allowed to contact the object, then those bodies will usurp a portion of the control over the object's motion. Therefore the first goal in grasping is to manipulate the object so that it loses all contact with the support. For this to be possible, the object must be *liftable*. The notion of liftability is a generalization of tippability, which is discussed elsewhere (Trinkle 1988).

> **Definition:** An object is *liftable* if and only if there exist finger contact positions on its surface for which increasing the magnitudes of the internal grasp forces (i.e., squeezing) applied by the fingers initiates motion, causing at least one of the supporting contacts to break.

In this definition of *liftability regions*, we focus on lifting by manipulation with sliding contacts; we are not concerned with the possibility that the object may be lifted by a hand using a non-sliding, force closure grasp achievable on accessible portions of the object's surface. Previous research results may be applied to this problem in a straightforward manner (Nguyen 1986).

2 Liftability Regions of Frictionless Planar Objects

Liftability regions define the qualitative motion of a squeezed object (i.e., rotate left, rotate right, translate, or jam) based on the geometry of the grasp. To determine these regions, we need a contact model that accurately represents the kinematic constraints and the appropriate limiting cases of the contact force distributions that identify the qualitative motion. The exact force distribution of a contact region is irrelevant. A model that satisfies these requirements is to consider all contacts as a set of one or more point contacts. A contact of small area is considered to be a single point.

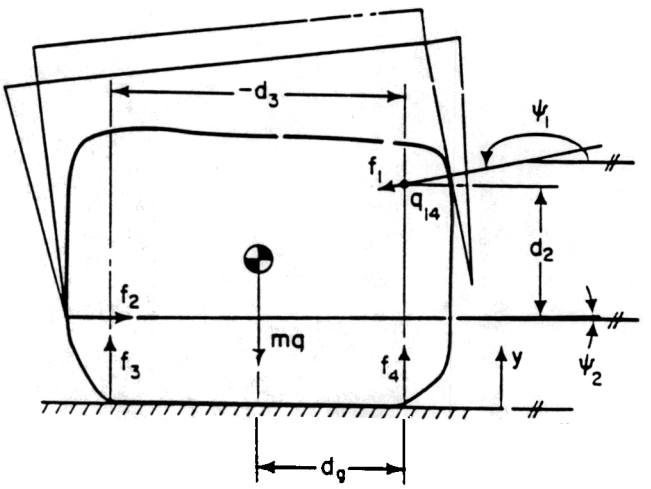

One with a large planar area is approximated by the set of points defining the vertices of the convex hull of the contact. Curved contact areas can be approximated by several polygons. During the following development, objects are assumed to be two-dimensional. However, any three-dimensional object that can be approximated as a generalized cylinder can be analyzed by our method by considering a suitable cross section of the cylinder.

Consider the two-point initial grasp of the frictionless, rigid, planar object depicted in Figure 1. The forces acting on the object are the finger contact forces ($\mathbf{f}_1$ and $\mathbf{f}_2$), the supporting contact forces ($\mathbf{f}_3$ and $\mathbf{f}_4$), and the weight of the object ($m\mathbf{g}$).

Under quasi-static conditions, the object must always satisfy the equilibrium relationships, which may be written as

$$\mathbf{W}\,\mathbf{c} = -\mathbf{g}_{ext} \tag{1}$$

$$\mathbf{c} \geq 0, \tag{2}$$

where equation (1) may be expanded as follows:

$$\begin{bmatrix} \hat{\mathbf{n}}_1 & \hat{\mathbf{n}}_2 & \hat{\mathbf{n}}_3 & \hat{\mathbf{n}}_4 \\ d_1 & d_2 & d_3 & d_4 \end{bmatrix} \begin{bmatrix} c_1 \\ c_2 \\ c_3 \\ c_4 \end{bmatrix} = -mg \begin{bmatrix} \hat{\mathbf{n}}_g \\ d_g \end{bmatrix}$$

$$d_i = \mathbf{r}_i \times \hat{\mathbf{n}}_i; \qquad i = \qquad , 4,$$

where W is the (3 × 4) wrench matrix, c is the vector of wrench intensities, $\mathbf{g}_{ext}$ is the external wrench (i.e., force and moment) (Ohwovoriole 1980) acting on the object, $\hat{\mathbf{n}}_i$ is the ith contact's unit normal vector directed inward with respect to the object, $\hat{\mathbf{n}}_g$ is the direction in which the external force acts on the object, d_i is the moment arm of the ith contact normal measured with respect to the summing point $\mathbf{q}_{14}$, which is defined by the intersections of $\hat{\mathbf{n}}_1$ and $\hat{\mathbf{n}}_4$, and d_g is the moment arm of the external force. The vector inequality (2) applies element by element. If we choose the external wrench $\mathbf{g}_{ext}$ to be that caused by gravity, the solution to equation (1) is given by

$$\begin{bmatrix} c_1 \\ c_2 \\ c_3 \\ c_4 \end{bmatrix} = \begin{bmatrix} 0 \\ 0 \\ c_{30} \\ c_{40} \end{bmatrix} + c_2 \begin{bmatrix} b_{21} \\ 1 \\ b_{23} \\ b_{24} \end{bmatrix} \tag{3}$$

where

$$c_{30} = \frac{mgd_g}{-d_3} > 0, \qquad c_{40} = \frac{mg(d_3 + d_g)}{d_3} > 0, \tag{4}$$

$$b_{21} = -\frac{\cos(\psi_2)}{\cos(\psi_1)} \qquad b_{23} = -\frac{d_2}{d_3}, \tag{5}$$

$$b_{24} = \frac{d_2}{d_3} + \frac{\sin(\psi_1 - \psi_2)}{\cos(\psi_1)} \tag{6}$$

ψ_i is the angle of the ith inward contact normal measured counterclockwise with respect to horizontal. Note that the second term on the right side of equation (3) is known as the internal grasping force (Salisbury 1982), because increasing c_2 increases the contact forces without changing the total force applied to the object.

To lift the object by squeezing, either c_3 or c_4 must be reduced to zero by increasing c_1 and c_2. The first row of equation (3) implies that for c_1 to increase with c_2, the following inequalities must hold:

$$\cos\psi_1 < 0 \tag{7}$$

$$\cos\psi_2 > 0 \tag{8}$$

where without loss of generality, the first contact has arbitrarily been chosen to be on the right side of the object. If inequalities (7) and (8) are not simultaneously satisfied, then squeezing will result in an unstable grasp; the object will slide out of the grasp to the left. For c_3 or c_4 to be driven to zero, at least one of b_{23} and b_{24} must be negative. Equating the third and fourth rows of equation (3) to zero gives the values of c_2 required to break the third and fourth contacts, respectively

$$c_{23} = \frac{mgd_g}{-d_2} \tag{9}$$

$$c_{24} = \frac{-mg(d_3 + d_g)\cos(\psi_1)}{d_2\cos(\psi_1) + d_3\sin(\psi_1 - \psi_2)} \tag{10}$$

Since c_2 is increased gradually after achieving the initial grasp, the contact that will break is the one corresponding to the smaller nonnegative value of c_2 [negative values of c_2 violate inequality (2)]. Thus equations (9) and (10) with inequalities (7) and (8) can be used to predict the motion caused by squeezing for every possible grasping configuration.

The magnitudes c_{23} and c_{24} depend on the grasp parameters ψ_1, ψ_2, and d_2. If we fix the position of the first finger's contact, then ψ_1 is constant, and ψ_2 and d_2 vary. Considering all possible contact points (and angles at vertices) for the second finger, the perimeter P may be partitioned into five mutually exclusive *liftability regions* S, J, $B3$, $B4$, and T that satisfy the following relationship:

$$S \cup J \cup B3 \cup B4 \cup T = P. \tag{1}$$

These regions correspond to possible contact points for the second finger for which squeezing causes the object to: slide along the support (S); jam the fingers (J), resulting in the object's being pressed against the support; tip, breaking the third contact ($B3$); tip, breaking the fourth contact ($B4$); and translate (T) or rotate, breaking the third and fourth contacts simultaneously. Figure 2 shows the liftability regions using a coded curve offset from the perimeter of the object. The codes corresponding to S, J, $B3$, $B4$, and T are: dashed curve, no curve, solid bold curve, thin solid curve, and double-bold solid curve. In Figure 2 the

Fig. 2. Liftability regions.

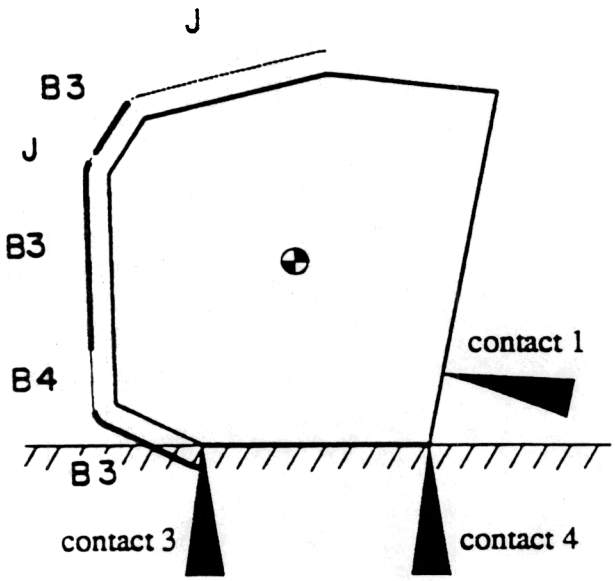

translation region is a set of distinct points, so no double-bold curve segments are visible.

2.2. Liftability Regions of Frictionless Polygons

A polygon can be used to approximate any two-dimensional object with arbitrary precision. Therefore we discuss the liftability regions of polygons in detail and then show how the results can be applied to curved objects.

The sliding region S is the portion of the perimeter for which the inward normal of the second contact has either no horizontal component or has a horizontal component with the same sense as that of $\mathbf{f}_1$. In Figure 3, S is comprised of edges 0, 1, 2, and 3; vertices 1, 2, and 3; and a portion of vertex 4.[1] If the second finger contacts the polygon in S, squeezing will cause sliding to the left.

The regions J, $B3$, $B4$, and T are partitions of the remaining perimeter denoted by S'. Consider the kth edge of the polygon in Figure 3. Points $\mathbf{p}$ lying on the

[1] What is meant by a portion of a vertex will be made clear later.

Fig. 3. Quantities for edge liftability regions.

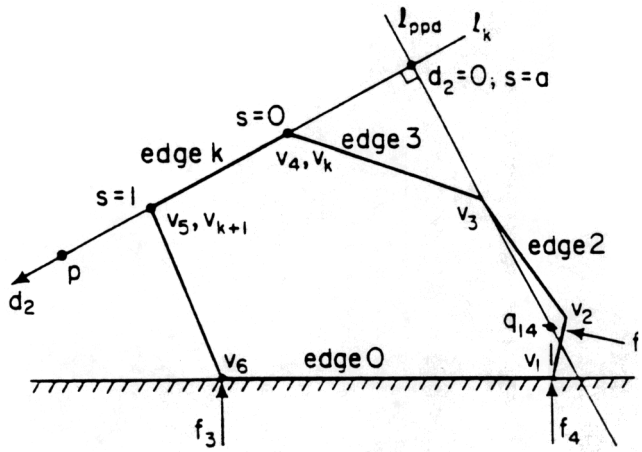

line l_k containing the edge can be written in parametric form as

$$(1 - s)\mathbf{v}_k + s\mathbf{v}_{k+1} = \mathbf{p} \tag{12}$$

where $\mathbf{v}_i$ represents the ith vertex of the polygon and the kth edge is defined by $s \in [0, 1]$. The line l_{ppd} is the unique line that is perpendicular to l_k and contains the point $\mathbf{q}_{14}$. The intersection of l_{ppd} with the kth edge defines the contact point where d_2, the moment arm of the second contact force, is zero. The variables s and d_2 are linearly related by

$$d_2 = s - a, \tag{13}$$

where a is the value of s at the intersection of l_k and l_{ppd}. Since d_2 varies linearly along the edge, c_{23} and c_{24} describe hyperbolas along l_k as shown in Figure 4. Note that the vertical asymptote of c_{24} is located at a positive value of d_2. This is the case defined by the following inequality:

$$\sin(\psi_1 - \psi_2) < 0. \tag{14}$$

When inequality (14) is satisfied, a *jamming region* J lies between the vertical asymptotes of the two hyperbolas, and the *jamming window* JW is the closed line segment $[\mathbf{q}_{13}, \mathbf{q}_{14}]$. The *breaking regions* $B3$ *and* $B4$ lie to the right and left of the jamming region. Since the values of c_{23} and c_{24} are not equal at any point on the edge, the *translation region* T is empty, implying that translational lifting is impossible if the second

Fig. 4. Formation of edge regions B3, B4, and J.

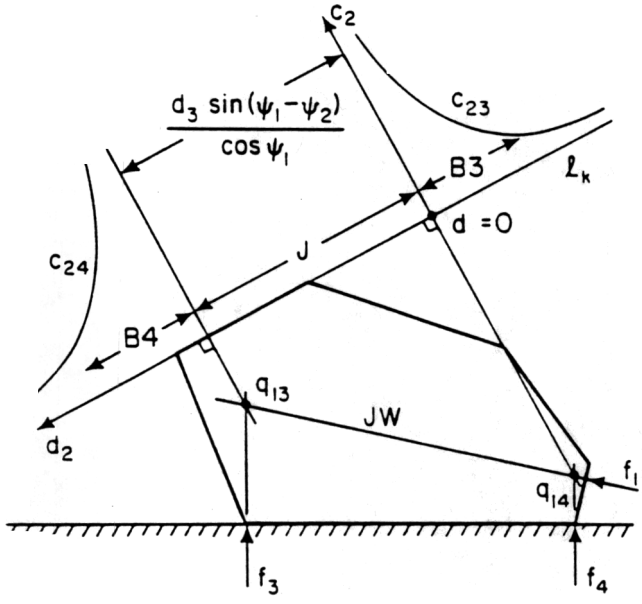

Fig. 5. Formation of edge regions B3, B4, and T.

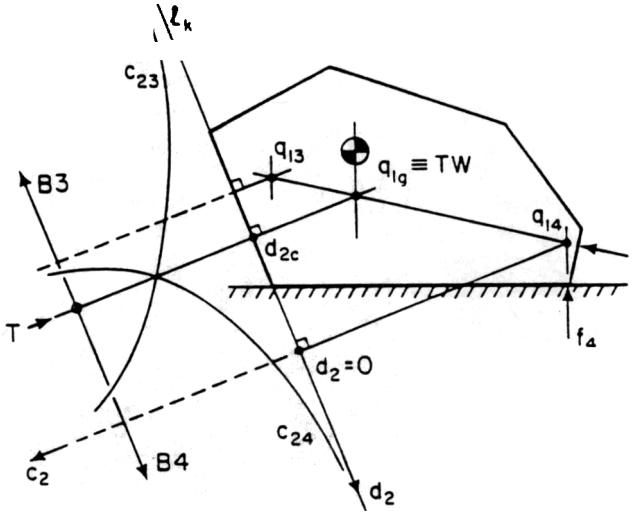

Fig. 6. Vertex liftability regions.

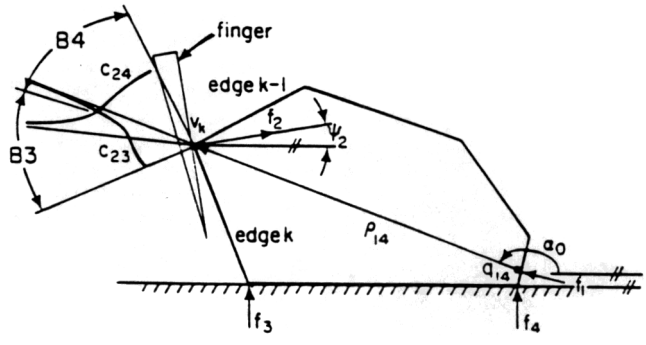

finger contacts that edge. Note that the physical significance of inequality (14) is that the resultant of the finger contact forces is in the direction of the gravity force. Therefore, to avoid jamming and to cause tipping, one must push down on the edge at a suitable point.

If the sense of inequality (14) is reversed,

$$\sin(\psi_1 - \psi_2) > 0,$$

then the functions c_{23} and c_{24} overlap, eliminating the jamming region (Fig. 5). The regions $B3$ and $B4$ meet at the crossover point d_{2c}:

$$d_{2c} = \frac{d_g \sin(\psi_1 - \psi_2)}{\cos(\psi_1)} \tag{16}$$

For the edge in question, d_{2c} is the only point that is an element of T. The contact normal from the point d_{2c} passes through the point $\mathbf{q}_{1g}$, called the *translation window TW*. If inequality (15) is satisfied, then the resultant of the finger's contact forces opposes gravity. Therefore, as the hand squeezes more and more tightly, the object must rise, because its weight is overcome.

The second contact point need not occur on an edge of the polygon. It may occur on the kth vertex, in which case the contact angle ψ_2 is free to vary between the inward normals of edges k and $k-1$ (Fig. 6), so that d_2 varies according to

$$d_2 = |\rho_{14}| \sin(\alpha_0 - \psi_2), \tag{17}$$

where the vector ρ_{14} is the position of the second contact point with respect to $\mathbf{q}_{14}$, and α_0 is the angle of ρ_{14} measured counterclockwise with respect to horizontal. Substituting equation (17) into equations (9) and (10) allows one to determine the liftability regions of a vertex. Figure 6 shows the edge of the second finger against the kth vertex in the region $B3$. Examination of the polar plots of c_{23} and c_{24} allows one to see that rotating the finger clockwise or counterclockwise

Fig. 7. Liftability regions of an edge.

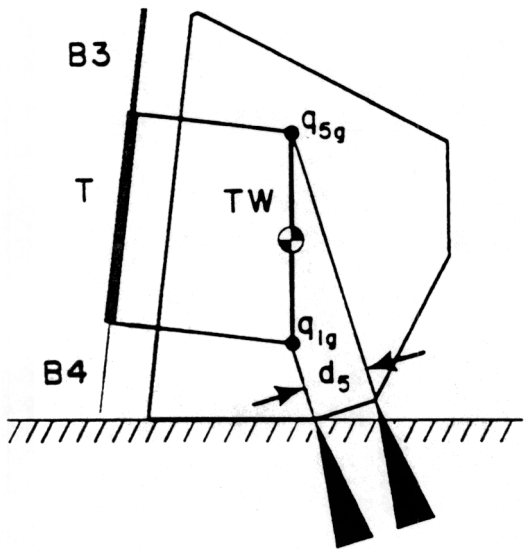

places the contact in region $B4$. Thus for a vertex, the liftability regions are defined as partitions of the range of possible contact normal angles.

2.3. Translational Liftoff

The first goal during dexterous manipulation is to break all contact with the support. Therefore it makes sense to use the translation region in planning the initial grasp. With only two finger contacts, the translation region is a set of distinct points and is impossible to contact (practically speaking).[2] However, a three-point initial grasp generates a translation region with finite length, making its use practical.

One way to achieve a third finger contact is by laying a finger against an edge of the polygon. This condition is indicated by two solid black triangles denoting two points of contact on a single edge (Fig. 7). Equilibrium equation (1) becomes

$$\mathbf{W}\,\mathbf{c} = -\mathbf{g}_{ex} \tag{1}$$

$$\begin{bmatrix} \hat{\mathbf{n}}_1 & \hat{\mathbf{n}}_2 & \hat{\mathbf{n}}_3 & \hat{\mathbf{n}}_4 & \hat{\mathbf{n}}_5 \\ d_1 & d_2 & d_3 & d_4 & d_5 \end{bmatrix} \begin{bmatrix} c_1 \\ c_2 \\ c_3 \\ c_4 \\ c_5 \end{bmatrix} = -mg \begin{bmatrix} \hat{\mathbf{n}}_g \\ d_g \end{bmatrix}$$

$$d_i = \mathbf{r}_i \times \hat{\mathbf{n}}_i; \qquad u = \qquad , 5.$$

The particular solution of equation (1) in which we are interested is the one for which the third and fourth contacts break, and the first, second, and fifth contacts are maintained. These conditions can be stated as

$$c_3 = 0 \quad c_4 = 0 \qquad c_1 > 0 \quad c_2 > 0 \quad c_5 > 0.$$

Removing the third and fourth columns from $\mathbf{W}$ and noting that $\psi_1 = \psi_5$ and $\hat{\mathbf{n}}_3 = \hat{\mathbf{n}}_4 = -\hat{\mathbf{n}}_g$, equation (1) can be solved for the type of initial grasp shown in Figure 7. Substituting the result into inequality (18) yields

$$\sin(\psi_1 \quad \psi_2) > 0$$

$$d_5 > 0$$

$$\frac{d_g \sin(\psi_1 - \psi_2)}{\cos(\psi_1)} + \frac{d_5 \cos(\psi_2)}{\cos(\psi_1)} < d_2 < \frac{d_g \sin(\psi_1 - \psi_2)}{\cos(\psi_1)} < 0.$$

Inequalities (19)[3] and (20) are necessary conditions for translation. We observe that inequality (20) can always be satisfied by suitably numbering the contact points. However, inequality (19) can only be satisfied by contacting the polygon on certain edges or portions of vertices. Inequality (21) defines the translation region T in which squeezing with the second finger causes the object to translate along the first finger breaking both support contacts. This region consists of

2. The points can be vertices of the polygon, but precise contact angles are required for translation. Positioning errors make it impossible to achieve the exact contact angles.

3. Note that inequality (19) is identical to inequality (15), which was seen above to be a necessary condition for translation with a two-point initial grasp.

Fig. 8. Liftability regions of a vertex.

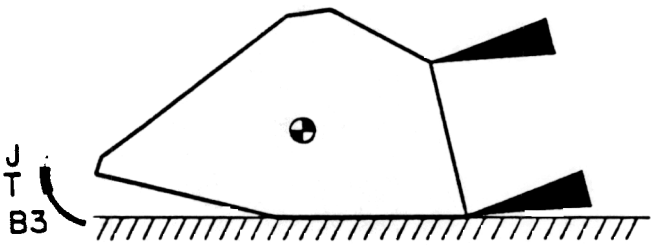

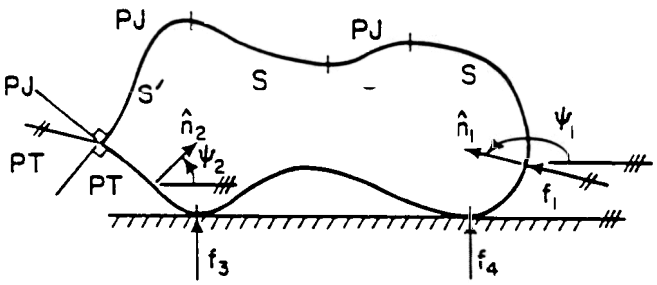

all points external to the sliding region S whose normals satisfy inequality (19) and pass through the translation window. The addition of the fifth contact has caused the translation window to grow from the point $\mathbf{q}_{1g}$ to the open line segment $(\mathbf{q}_{1g}, \mathbf{q}_{5g})$. Figure 7 illustrates the translation window TW and the translation region T (and $B3$ and $B4$) of one edge for a specific placement of the first finger. For a vertex, the translation region is determined by substituting equation (17) into inequality (21) (Fig. 8).

2.4. Graphical Construction of Liftability Regions

A graphical method to determine the liftability regions of any planar curve with or without vertices for two- and three-point initial grasps has been developed based on the above analysis. It is best to illustrate the method with the following example.

Two-Point Initial Grasps

First, the perimeter of the object is partioned into the complementary regions S and S' as shown inside the object's perimeter in Figure 9. The region S is the set

Fig. 9. Regions S *and* S′ *and* PT *and* PJ.

Fig. 10. Regions $B3_T$, $B4_T$, *and* T.

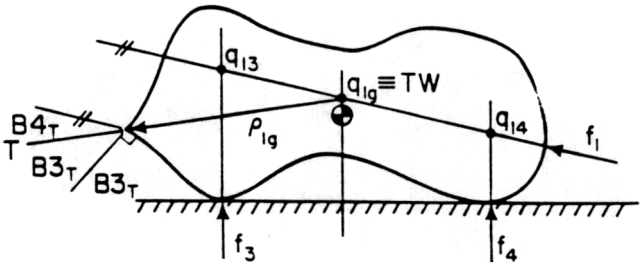

of points $\mathbf{p}$ for which all local contact normals have a nonpositive component in the x direction. The region S' is the set of points whose normals have positive x components.

$$S = \{\mathbf{p}: \quad \cos(\psi) \leq 0\}$$

$$S' = \{\mathbf{p}: \quad \cos(\psi) > 0\}$$

where the prime denotes the set complement operation.

Second, the first finger's contact is chosen to satisfy inequality (7) (i.e., the first contact point is in the interior of S). Therefore, to satisfy equilibrium relationships (1) and (2), the second finger's contact must be in S'. Next we divide S' into regions of possible translation PT and possible jamming PJ based on inequalities (14) and (19):

$$PT = \{\mathbf{p}: \quad \sin(\psi_1 - \psi_2) > 0 \text{ and } \mathbf{p} \in S'\}$$

$$PJ = \{\mathbf{p}: \quad \sin(\psi_1 - \psi_2) \leq 0 \text{ and } \mathbf{p} \in S'\}. \quad (25)$$

The partitions are shown outside the object's perimeter in Figure 9.

Third, we define the points $\mathbf{q}_{13}$, $\mathbf{q}_{14}$, and $\mathbf{q}_{1g}$. They are at the intersections of the lines of action of the third, fourth, and gravity forces, respectively, with the line of action of the first contact force (Fig. 10).

Fourth, the region PT is broken into $B3_T$, $B4_T$, and T. Points in PT whose contact normals pass through the translation window $\mathbf{q}_{1g}$ belong to T. Points whose normals produce positive or negative moments with respect to the translation window belong to $B4_T$ or $B3_T$, respectively (see Fig. 10):

$$B3_T = \{\mathbf{p}: \quad \rho_{1g} \times \hat{\mathbf{n}}_2 < 0 \text{ and } \mathbf{p} \in PT\} \quad (26)$$

$$B4_T = \{\mathbf{p}: \quad \rho_{1g} \times \hat{\mathbf{n}}_2 > 0 \text{ and } \mathbf{p} \in PT\} \quad (27)$$

Fig. 11. Regions $B3_J$, $B4_J$ and J.

Fig. 12. Liftability regions for a two-point initial grasp.

Fig. 13. Liftability regions for a three-point initial grasp.

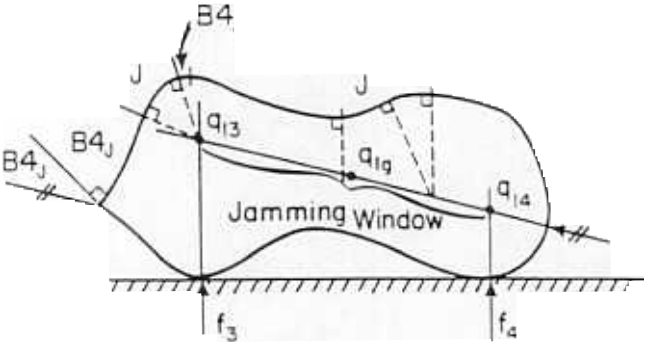

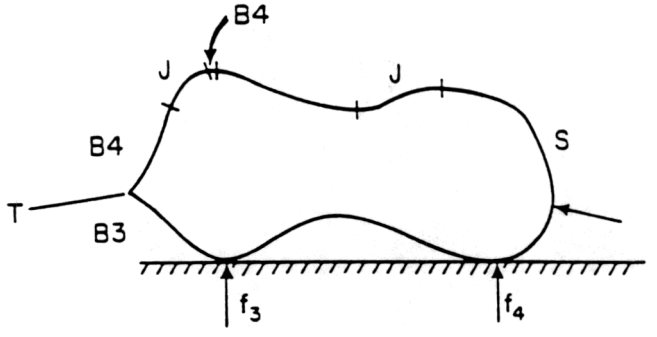

$$T = \{\mathbf{p}: \quad \rho_{1g} \times \hat{\mathbf{n}}_2 = 0 \text{ and } \mathbf{p} \in PT\} \tag{28}$$

where recall ρ_{ij} is the position of the second contact point relative to $\mathbf{q}_{ij}$, and $\hat{\mathbf{n}}_2$ is the normal unit vector of the second contact.

Fifth, PJ is divided into $B3_J$, $B4_J$, and J. Points in PJ whose contact normals intersect the jamming window $[\mathbf{q}_{13}, \mathbf{q}_{14}]$ are elements of J. The points whose normals do not intersect the jamming window and generate a positive or negative moment with respect to $\mathbf{q}_{1g}$ belong to region $B4_J$ or $B3_J$, respectively (Fig. 11).

$$B3_J = \{\mathbf{p}: \quad \rho_{14} \times \hat{\mathbf{n}}_2 < 0 \text{ and } \mathbf{p} \in PJ\} \tag{29}$$

$$B4_J = \{\mathbf{p}: \quad \rho_{13} \times \hat{\mathbf{n}}_2 > 0 \text{ and } \mathbf{p} \in PJ\} \tag{30}$$

$$J = \{\mathbf{p}: \quad \rho_{13} \times \hat{\mathbf{n}}_2 \leq 0 \text{ and } \rho_{14} \times \hat{\mathbf{n}}_2 \geq 0 \text{ and } \mathbf{p} \in PJ\} \tag{31}$$

Finally, the liftability regions J and T are complete. However, the regions $B3$ and $B4$ must be formed by the unions of the individual $B3$s and $B4$s found in steps 4 and 5.

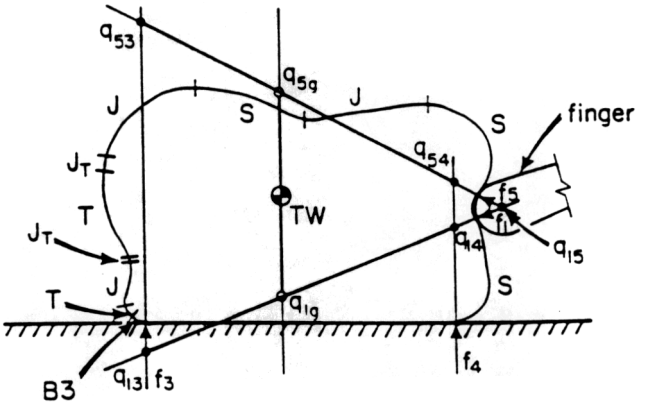

$$B3 = B3_T \cup B3_J \tag{32}$$

$$B4 = B4_T \cup B4_J.$$

Figure 12 shows the liftability regions. Note that by construction, the liftability regions are mutually exclusive and contain every point on the perimeter P.

Three-Point Initial Grasp

The liftability regions for a three-point initial grasp can be formed by combining the liftability regions corresponding to the two possible two-point initial grasps.[4] Let S_i, J_i, $B3_i$, $B4_i$, and T_i denote the liftability regions when considering only the ith contact; $i \in \{1, 5\}$. Denote by S, J, $B3$, $B4$, and T the liftability regions for the three-point grasp. In the appendix we show that the following relationships hold:

$$S = S_1 = S_5$$

$$J = J_1 \cup J_5 \cup J_T$$

$$B3 = B3_1 \cap B3_5$$

$$B4 = B4_1 \cap B4_5$$

$$T = (B3_1 \cap B4_5 \cap J_T') \cup (T_1 \cap B4_5) \cup (T_5 \cap B4_1)$$

4. There are three possible initial two-point grasps, one of which must cause the object to slide left or right.

Fig. 14. Liftability regions for two-point and three-point initial grasps of several polygons. Note that the object on the left does not develop a translation region.

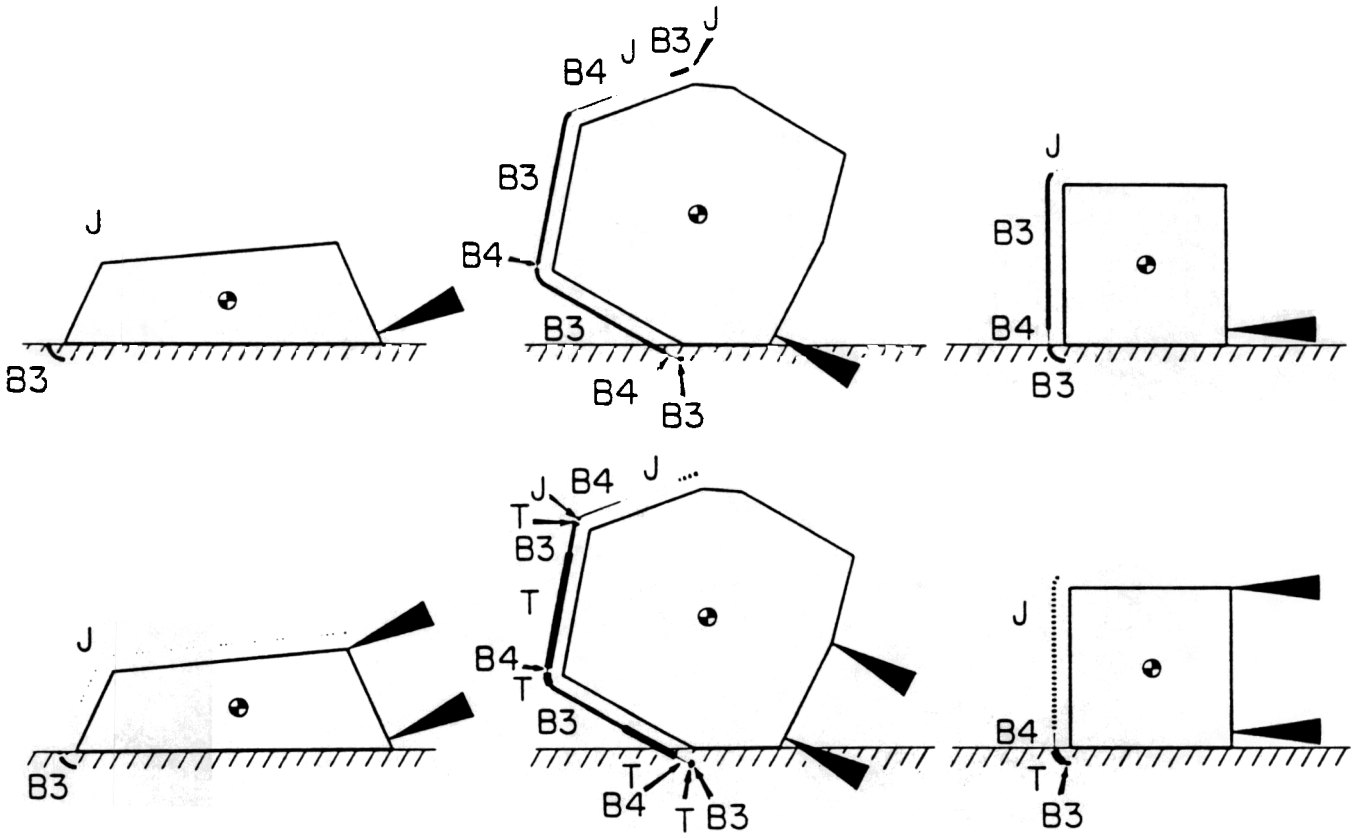

Equations (35)–(39) imply that the regions J and T grow at the expense of $B3$ and $B4$. Thus we see that including an extra contact point allows a grasp to be achieved in the translation region but leaves less of the perimeter available for tipping grasps.

The additional jamming region J_T and the new translation region T can be found graphically by using the new translation window $(\mathbf{q}_{1_g}, \mathbf{q}_{5_g})$ (Fig. 13). There are two cases: $\mathbf{q}_{15}$ on the right of the translation window and $\mathbf{q}_{15}$ on the left. For $\mathbf{q}_{15}$ on the right, the translation region consists of those points, elements of S', whose contact normals pass through the translation window and $(\mathbf{q}_{5_g}, \mathbf{q}_{15})$. The region J_T contains all points in S' whose normals pass through the translation window and $(\mathbf{q}_{14}, \mathbf{q}_{15})$. For $\mathbf{q}_{15}$ on the left, the translation region consists of the points in S' whose contact normals pass through the translation window and $(\mathbf{q}_{1_g}, \mathbf{q}_{15})$. The region J_T contains all points in S' whose normals pass through the translation window and $(\mathbf{q}_{15}, \mathbf{q}_{53})$. These facts can be used to find the most important liftability region, T, without computing all the liftability regions for both two-point grasps.

Figure 14 shows the positions of contacts 1 and 5 for several polygons. The perimeter of each object is grown and coded as described in the last paragraph of section 2.1. The first row of the figure shows the liftability regions for two-point initial grasps, and therefore no translation regions are visible. The second row shows the regions for three-point initial grasps. Note that translation regions have appeared, but the jamming regions have grown.

2.5. Liftability Regions with Friction

When friction is present, the method for computing the liftability regions becomes more complicated. However, a conservative subset of the translation re-

Fig. 15. Grasp in T with friction.

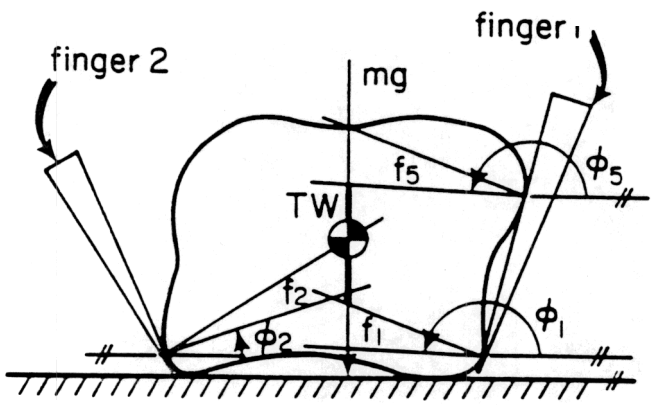

Fig. 16. Grasp force diagram.

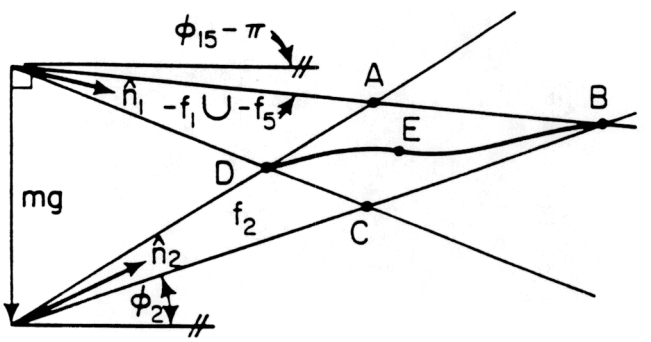

gion can be determined much like before. The translation window is the portion of the line of action of the gravitational force lying between the friction cones of the forces $\mathbf{f}_1$ and $\mathbf{f}_5$ as illustrated in Figure 15. The translation region consists of the points on the object's perimeter for which the cone of $\mathbf{f}_2$ is completely within the translation window. Under these conditions all finger contacts will be maintained during squeezing or releasing. As in the frictionless case, we can guarantee that the object will translate on finger 1 if the following sufficient conditions are met. First,

$$\sin(\phi_{15} - \phi_2) > 0 \tag{40}$$

where $\phi_{15} = \max(\phi_1, \phi_5)$, ϕ_1 and ϕ_5 are the angles of the counterclockwise-most edges of cones 1 and 5, and ϕ_2 is the angle of the clockwise-most edge of cone 2. Second, finger 2 contacts the object in the translation region. It may seem, because the translation region is smaller with friction than without, that lifting has become more difficult. However, the correct interpretation is that friction hinders (translational) sliding manipulation while facilitating lifting via grasps with rolling contacts.

Figure 16 shows a force diagram for the grasp depicted in Figure 15. The lower cone $\mathbf{f}_2$ corresponds to the possible forces acting at the second contact point. The upper cone represents all possible linear combinations of the forces generated at the other two contact points. The point E represents a particular combination of contact forces that result in the object's equilibrium. If E is on the interior of the quadrilateral $ABCD$, then the object remains fixed relative to the hand. As the internal grasp force is increased, the magnitude of $\mathbf{f}_2$ increases. Eventually E reaches the boundary AB, at which point the object begins sliding up finger 1. Alternatively, the internal grasp force could be reduced until the object slides down. Because sliding on finger 1 typically results in sliding on finger 2, it is expected that the trajectory of E will terminate at points B and D. If termination occurs on AB or CD, then the second finger's motion would be required to comply with that of the object. For example, if E lies on the interior of the line segment AB, then contacts 1 and 5 are sliding, because the contact forces $\mathbf{f}_1$ and $\mathbf{f}_5$ lie on the edge of their friction cone. However, contact force $\mathbf{f}_2$ lies within its cone, which implies that the second contact point on the object and finger must have identical velocities.

If inequality (40) is not satisfied, edges AB and BC become infinite, making it impossible to cause the object to slide up finger 1 by squeezing. An example of this situation occurs when the contacts are on parallel edges of an object. It should be noted, however, that edges AD and DC are always finite for stable grasps, which implies that an object will always slide out of the hand if the internal grasp force is reduced enough.

One remaining concern is that the boundaries AB and CD of the quadrilateral are conservative estimates. The cone $-(\mathbf{f}_1 \cup \mathbf{f}_5)$ allows for all possible combinations of the first and fifth contact forces. Since effects of deformation will determine the nature of load sharing between contacts 1 and 5, realistic boundaries AB and CD will be on the interior of the quadrilateral, so that the predicted internal grasp force to cause sliding will be greater than the actual value.

In planning, one must specify the intended motion of the object (i.e., up or down finger 1). Given this knowledge, the conservatively formed translation window may be expanded to the upper edge of the cone $\mathbf{f}_5$ for upward sliding or expanded to the lower edge of the cone $\mathbf{f}_2$ for downward sliding. If, in addition, one knows the intended contact velocity of finger 2, then the translation region may be determined by requiring the appropriate edge of the cone of $\mathbf{f}_2$ (rather than the entire cone) to pass through the translation window. Thus when translation manipulation is prespecified, the translation region is found as though the object were frictionless but with the contact normals rotated in the appropriate directions by the amounts of the friction angles.

The motion of the object for all other frictionless grasp configurations and finger motions can be predicted by solving the *forward object motion problem.* Trinkle (1987) found the velocity of a frictionless object as the solution of a linear program. It was determined that such an object will move to minimize its rate of gain of potential energy while adhering to the velocity constraints imposed by the fingers. The frictionless assumption is quite limiting but is successfully removed in the following section.

2.6. Forward Object Motion Problem with Coulomb Friction

The *forward object motion problem* can be extended to include Coulomb friction using Peshkin's minimum power principle (Peshkin and Sanderson 1989). Roughly speaking the ". . . minimum power principle states that a system chooses at every instant the lowest energy of 'easiest' motion in conformity with the constraints." This principle applies only to quasi-static systems subject to forces of constraint (i.e., normal forces), Coulomb friction forces, and forces independent of velocity. For this principle, the power is defined as

$$P_{xc} = -\sum_i \mathbf{f}_{xci} \cdot \mathbf{v}_i \qquad (41)$$

where $\mathbf{v}_i$ is the velocity of the ith point of application of external forces, and $\mathbf{f}_{xci}$ is the sum of the external forces, excluding constraint forces, applied to the ith point. Included in P_{xc} are the friction and gravitational forces. The normal forces at the contacts are omitted. Thus P_{xc} is only a fraction of the object's power.

The wrench $\mathbf{w}_i$, applied to the object through the ith point contact with friction, can be written as the product of the ith contact's unit wrench matrix $\mathbf{W}_i$ and the wrench intensity vector $\mathbf{c}_i$,

$$\mathbf{w}_i = \mathbf{W}_i \mathbf{c}_i; \qquad i = \qquad , n_c,$$

where n_c is the number of contact points,

$$\mathbf{W}_i = \begin{bmatrix} \hat{\mathbf{t}}_i & \hat{\mathbf{o}}_i & \hat{\mathbf{n}}_i \\ \mathbf{r}_i \times \hat{\mathbf{t}}_i & \mathbf{r}_i \times \hat{\mathbf{o}}_i & \mathbf{r}_i \times \hat{\mathbf{n}}_i \end{bmatrix}, \qquad \mathbf{c}_i = \begin{bmatrix} c_{it} \\ c_{io} \\ c_{in} \end{bmatrix}, \quad (43)$$

$\mathbf{r}_i$ is the position of the ith contact point, $\hat{\mathbf{n}}_i$ is the contact's unit normal directed inward with respect to the object, $\hat{\mathbf{t}}_i$ and $\hat{\mathbf{o}}_i$ are orthogonal unit vectors defining the contact tangent plane, and the elements of $\mathbf{c}_i$ are the components of the ith contact force in the $\hat{\mathbf{t}}_i$, $\hat{\mathbf{o}}i$, and $\hat{\mathbf{n}}_i$ directions. Including all contacts, the equilibrium equation (1) can be partitioned as follows:

$$[\mathbf{W}_t \quad \mathbf{W}_o \quad \mathbf{W}_n] \begin{bmatrix} \mathbf{c}_t \\ \mathbf{c}_o \\ \mathbf{c}_n \end{bmatrix} = -\mathbf{g}_{ext}$$

where

$$\mathbf{W}_n = \begin{bmatrix} \hat{\mathbf{n}}_1 & \hat{\mathbf{n}}_2 & \cdots & \hat{\mathbf{n}}_{n_c} \\ \mathbf{r}_1 \times \hat{\mathbf{n}}_1 & \mathbf{r}_2 \times \hat{\mathbf{n}}_2 & \cdots & \mathbf{r}_{n_c} \times \hat{\mathbf{n}}_{n_c} \end{bmatrix} \qquad \mathbf{c}_n = \begin{bmatrix} \\ \\ \\ c_{n_c n} \end{bmatrix}$$

with $\mathbf{W}_o$, $\mathbf{W}_t$, $\mathbf{c}_o$, and $\mathbf{c}_t$ defined in parallel fashion. The above partitioning of the wrench matrix allows us to write the sum of the friction wrenches as $\mathbf{W}_t\ \mathbf{c}_t + \mathbf{W}_o\ \mathbf{c}_o$ and the sum of the contact normal wrenches as $\mathbf{W}_n\ \mathbf{c}_n$. We now form the equation for the power as follows:

$$P_{xc} = -\dot{\mathbf{q}}_{ob}{}^{\mathrm{T}} \left\{ \mathbf{g}_{ext} + [\mathbf{W}_t \quad \mathbf{W}_o] \begin{bmatrix} \mathbf{c}_t \\ \mathbf{c}_o \end{bmatrix} \right\},$$

where $\dot{\mathbf{q}}_{ob}$ represents the object's linear and angular velocities and the superscript $^{\mathrm{T}}$ denotes matrix transposition. Given the joint velocities of the hand and arm, $\dot{\theta}$, the velocity of the object may be found by minimizing P_{xc} subject to the rigid body velocity constraints and the Coulomb friction constraints. The velocity constraints disallow interference between rigid bodies and may be written as

$$\mathbf{W}_n^{\mathrm{T}}\dot{\mathbf{q}}_{ob} \geq \mathbf{J}_n\ \dot{\theta}, \tag{47}$$

where $\mathbf{J}_n$ is the partition of the global grasp Jacobian [Kerr 1984; also called the global transmitted grasp Jacobian (Trinkle 1987)] corresponding to the normal components of the contact velocities, and $\mathbf{W}_n^{\mathrm{T}}\ \dot{\mathbf{q}}_{ob}$ and $\mathbf{J}_n\ \dot{\theta}$ are the vectors of the normal velocity components of the contact points on the object and the hand, respectively.

The Coulomb friction constraints require that the ith contact force lie within the friction cone given by

$$c_{it}^2 + c_{io}^2 \leq \mu_i^2\ c_{in}^2; \qquad i = 1, \qquad , n_c \tag{48}$$

$$c_{in} \geq 0; \qquad i = \qquad , n_c \tag{49}$$

where μ_i is the coefficient of friction acting at the ith contact point. Inequality (48) may be written in matrix form as follows

$$\mathbf{c}_i^T\ \mathbf{D}_i\ \mathbf{c}_i \geq 0; \qquad i = \qquad , n_c \tag{50}$$

where

$$\mathbf{D}_i = \begin{bmatrix} -1 & 0 & 0 \\ 0 & -1 & 0 \\ 0 & 0 & \mu_i^2 \end{bmatrix} \tag{51}$$

Application of the minimum power principle requires that P_{xc} be minimized subject to inequalities (47), (49), and (50). One might think that the equilibrium equation (1) should also be used to constrain the minimization. However, by formulating and examining the dual optimization problem, one finds that equilibrium equation (1) is implicitly satisfied and that inequality (49) is redundant. Thus the primal problem is given by

$$\text{Minimize} \quad P_{xc} = -\dot{\mathbf{q}}_{ob}^{\mathrm{T}}\left\{\mathbf{g}_{ext} + [\mathbf{W}_t\ \mathbf{W}_o]\begin{bmatrix}\mathbf{c}_t \\ \mathbf{c}_o\end{bmatrix}\right\} \tag{46}$$

$$\text{Subject to:} \quad \mathbf{W}_n^{\mathrm{T}}\ \dot{\mathbf{q}}_{ob} \geq \mathbf{J}_n\ \dot{\theta} \tag{47}$$

$$\mathbf{c}_i^{\mathrm{T}}\ \mathbf{D}_i\ \mathbf{c}_i \geq 0; \qquad i = \qquad , n_c$$

with unknowns $\dot{\mathbf{q}}_{ob}$, $\mathbf{c}_t$, $\mathbf{c}_o$ and $\mathbf{c}_n$ (implicit in the vectors $\mathbf{c}_i$).

Applying the Kuhn-Tucker optimality conditions (Beveridge and Schechter 1970) to the primal problem yields the dual constraints. The dual objective function is derived by substituting the velocity constraints into the primal objective function and considering the implications of maximizing the result. After some manipulation, the dual problem is seen to be

$$\text{Maximize} \quad P_c = \theta^{\mathrm{T}}\mathbf{J}_n\ \lambda$$

$$\text{Subject to:} \quad \mathbf{g}_{ext} + [\mathbf{W}_t\ \ \mathbf{W}_o]\begin{bmatrix}\mathbf{c}_t \\ \mathbf{c}_o\end{bmatrix} + \mathbf{W}_n\lambda = 0$$

$$\mathbf{W}_t^{\mathrm{T}}\ \dot{\mathbf{q}}_{ob} + 2\,\mathbf{N}^{\mathrm{T}}\ \mathbf{D}_t\ \mathbf{c}_t = 0 \tag{54}$$

$$\mathbf{W}_o^{\mathrm{T}}\ \dot{\mathbf{q}}_{ob} + 2\,\mathbf{N}^{\mathrm{T}}\ \mathbf{D}_o\ \mathbf{c}_o = 0 \tag{55}$$

$$2\,\mathbf{N}^{\mathrm{T}}\ \mathbf{D}_n\ \mathbf{c}_n = 0 \tag{56}$$

$$\lambda \geq 0 \tag{57}$$

$$\eta \geq 0 \tag{58}$$

where λ is the vector of Lagrange multipliers associated with inequality (47), $\mathbf{N}$ is a diagonal matrix whose nonzero elements are the Lagrange multipliers η_i associated with inequalities (50), $\mathbf{D}_t$ and $\mathbf{D}_o$ are identity matrices, and $\mathbf{D}_n$ is a diagonal matrix with nonzero elements given by $-\mu_i^2$. It is well known that the value of the Lagrange multiplier associated with a specific rigid contact constraint is equal to the magnitude of the normal force necessary to maintain contact (Lanczos 1986). Therefore the vector λ is equivalent to $\mathbf{c}_n$, and it is evident that constraint (53) is equivalent to the equilibrium equation (1), and constraint (57) is equivalent to inequality (49).

At the optimal solution, both the primal constraints and the dual constraints are satisfied; therefore the

primal problem defined by the nonlinear program, (46), (47), and (50), need not include the equilibrium equation. Another interesting point is that for all feasible solutions, the primal and dual objective functions satisfy the following relationship

$$\dot{\theta}^T \mathbf{J}_n^T \mathbf{c}_n \leq -\dot{\mathbf{q}}_{ob}^T \mathbf{g}_{ext} - \dot{\mathbf{q}}_{ob}^T [\mathbf{W}_t \quad \mathbf{W}_o] \begin{bmatrix} \mathbf{c}_t \\ \mathbf{c}_o \end{bmatrix}, \quad (59)$$

with equality holding only at the optimal solution. The term on the left side of the inequality is the power applied to the object by the forces of constraint. The terms on the right are the rate of gain of potential energy and the power dissipation through Coulomb friction. Thus at the optimal solution, expression (59) has the following physical interpretation. The motion of the fingers in the direction of the contact normals supplies power to the object. Some of that power is lost to friction. What remains goes into lifting the object. Consequently every suboptimal solution must defy conservation of energy.

2.7. Extension: Sliding Contacts

The primal forward object motion problem (46), (47), and (50) is complete for rolling contacts but not for sliding contacts. If sliding occurs at the ith contact, then the ith inequality in (47) and inequality (50) must be satisfied as equalities. The former implies the sliding condition, and the latter requires the contact force to lie on the boundary of the friction cone. The Coulomb model of friction also specifies that the contact force be anti-parallel to the relative contact velocity. This specification was concisely expressed by Jameson (1985) as

$$\mathbf{c}_i \cdot ({}^C\mathbf{v}_{ri} \times \hat{\mathbf{n}}_i) = 0; \qquad i = 1, \ldots, n_c \quad (60)$$

$$\mathbf{c}_i \cdot {}^C\mathbf{v}_{ri} \leq 0; \qquad i = 1, \ldots, n_c \quad (61)$$

where ${}^C\mathbf{v}_{ri}$ is the relative contact velocity (or simply contact velocity) expressed with respect to the ith contact frame. Constraint (60) requires that contact force to lie in the plane formed by the sliding velocity vector and the contact normal. Constraint (61) implies that the friction force opposes the contact velocity, thereby dissipating power. The contact velocity is given by

$${}^C\mathbf{v}_{ri} = \mathbf{W}_i^T \dot{\mathbf{q}}_{ob} - \mathbf{J}_i \dot{\theta}; \qquad i = 1, \ldots, n_c, \quad (62)$$

where $\mathbf{J}_i$ is the transmitted Jacobian of the ith contact (Trinkle 1987). Relations (60) and (61) may be written in terms of the wrench intensities and the object and arm velocities as the following set of nonsmooth, nonconvex constraints

$$\mathbf{c}_i^T \mathbf{A}_i \mathbf{W}_i^T \dot{\mathbf{q}}_{ob} - \mathbf{c}_i^T \mathbf{A}_i \mathbf{J}_i \dot{\theta} = 0; \qquad i = \quad , \ldots, n_c \quad (63)$$

$$\mathbf{c}_i^T \mathbf{W}_i^T \dot{\mathbf{q}}_{ob} - \mathbf{c}_i^T \mathbf{J}_i \dot{\theta} \leq 0; \qquad i = 1, \quad , \ldots, n_c \quad (64)$$

where $\mathbf{A}_i$ is the skew-symmetric cross product matrix associated with the unit normal at the ith contact $\hat{\mathbf{n}}_i$.

The complete primal problem is now given by

$$\text{Minimize} \quad P_{xc} = -\dot{\mathbf{q}}_{ob}^T \left\{ \mathbf{g}_{ext} + [\mathbf{W}_t \quad \mathbf{W}_o] \begin{bmatrix} \mathbf{c}_t \\ \mathbf{c}_o \end{bmatrix} \right\} \quad (46)$$

$$\text{Subject to:} \qquad \mathbf{W}_n^T \dot{\mathbf{q}}_{ob} \geq \mathbf{J}_n \dot{\theta} \quad (47)$$

$$\mathbf{c}_i^T \mathbf{D}_i \mathbf{c}_i \geq 0; \qquad i \in \Omega \quad (50)$$

$$\mathbf{c}_i^T \mathbf{A}_i \mathbf{W}_i^T \dot{\mathbf{q}}_{ob} - \mathbf{c}_i^T \mathbf{A}_i \mathbf{J}_i \dot{\theta} = 0; \qquad i \in \Psi \quad (63)$$

$$\mathbf{c}_i^T \mathbf{W}_i^T \dot{\mathbf{q}}_{ob} - \mathbf{c}_i^T \mathbf{J}_i \dot{\theta} \leq 0; \qquad i \in \Psi \quad (64)$$

where Ω and Ψ represent the set of contact points assumed to be maintained and sliding, respectively. More precisely, we write

$$\Omega = \{i \quad \mathbf{w}_{ni}^T \dot{\mathbf{q}}_{ob} = \mathbf{j}_{ni}^T \dot{\theta}\}$$

$$\Psi = \{i \quad i \in \Omega \cap \mathbf{c}_i^T \mathbf{D}_i \mathbf{c}_i = 0\}$$

where $\mathbf{w}_{ni}^T$ is the ith row of $\mathbf{W}_n^T$, and $\mathbf{j}_{ni}^T$ is the ith row of $\mathbf{J}_n$. Constraints (63) and (64) complete the Coulomb friction model without which friction forces could create rather than dissipate power, resulting in an unbounded objective function.

To determine $\dot{\mathbf{q}}_{ob}$, P_{xc} must be minimized subject to the rigid body velocity constraints (47) and the Coulomb friction constraints (50), (63), and (64). The object will execute the motion corresponding to the

feasible solution of least power. If no feasible solution exists, then the proposed motion of the robot is kinematically inadmissible (i.e., the mechanism will jam). If the minimum power solution is unbounded, then the proposed motion causes the grasp configuration to become unstable (i.e., danger of dropping the object is imminent).

Clearly the general *forward object motion problem* depends not only on the grasp configuration but also on the velocities of the contacts. Therefore it is not possible to define liftability regions and use them in planning. Each grasp and desired vector of joint velocities must be considered separately.

2.8. Special Case: Frictionless Contacts

The *forward object motion problem* given above reduces to a linear program when friction is absent. This simplification may be seen by noting that the only nonlinear constraints, (50), (63), and (64), are removed, because they are a result of the Coulomb friction model. In addition, since friction forces no longer dissipate power, the second term in the primal object function (and the associated variables $\mathbf{c}_n$ and $\mathbf{c}_o$) becomes zero. Thus in the frictionless case, the primal forward object motion problem reduces to the following single linear program, called the *velocity formulation* of the frictionless object motion problem:

$$\text{Minimize} \quad P_{xc} = -\dot{\mathbf{q}}_{ob}^{\mathsf{T}}\, \mathbf{g}_{ext} \tag{65}$$

$$\text{Subject to:} \quad \mathbf{W}_n^{\mathsf{T}}\, \dot{\mathbf{q}}_{ob} \geq \mathbf{J}_n\, \dot{\theta}. \tag{47}$$

The input of this formulation is, as before, the vector of joint velocities of the robot. Its output is the contact forces [i.e., the Lagrange multipliers associated with inequality (47)], the velocity of the object, and the nature of the contact interactions. The contact interactions are indicated by the values of the Lagrange multipliers: if the ith multiplier is zero, then the bodies are separating at the ith contact; if the ith multiplier is positive, then the bodies are sliding on one another at the ith contact; negative values of the multipliers are impossible. Note that this linear program (derived beginning with Peshkin's minimum power principle) is identical to that derived by Trinkle (1987), who began with the assumption that a manipulated frictionless object would move upward as little as possible.

The dual linear program is called the *force formulation* of the frictionless object motion problem and is stated as follows:

$$\text{Maximize} \quad P_c = \dot{\theta}^{\mathsf{T}}\, \mathbf{J}_n\, \mathbf{c}_n$$

$$\text{Subject to:} \quad \mathbf{g}_{ext} + \mathbf{W}_n\, \mathbf{c}_n = 0$$

$$\mathbf{c}_n \geq 0.$$

The velocity and force formulations are equivalent, and therefore the input-output relationship for the dual is identical to that of the primal. As was the case for the formulations with friction, the primal and dual solutions are equivalent at the optimal solution so that energy is conserved.

3. Manipulation Planning

The ultimate goal of our analysis is to provide a framework in which intelligent dexterous manipulation can be planned for articulated mechanical hands. Intelligent dexterous manipulation can be considered to be the continuous evolution of a stable grasp from an undesirable configuration to one appropriate to the performance of a given task. The simplest task is a pick-and-place operation, which can be easily performed with a parallel-jawed gripper if friction is significant. However, such a gripper is useless in the frictionless case. To hold an object without friction requires that the hand envelop the object much as one would grip a wet piece of ice. Therefore under slippery conditions an articulated hand is necessary.

Figure 17(A) shows the simplest two-dimensional articulated hand performing an enveloping grasp [also called a form closure grasp (Lakshminarayana 1978)] of a frictionless object. For the remainder of this article, objects are considered to be convex frictionless polygons, and the hand is assumed to be the one pictured in Figure 17.

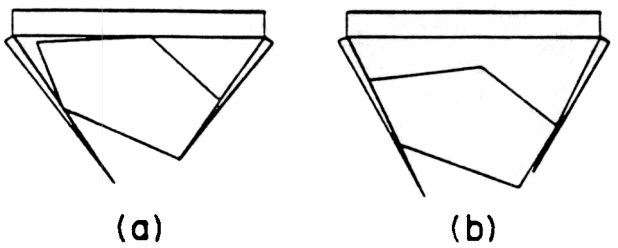

Fig. 17. A, *A form closure grasp of the object.* B, *A typical force closure grasp.*

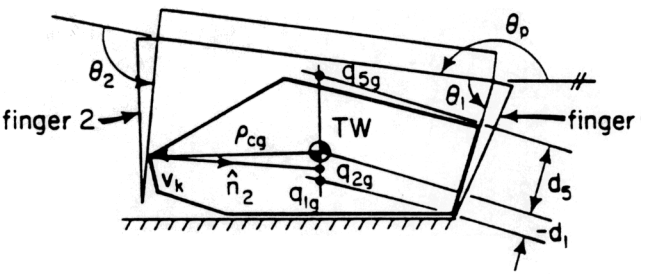

Fig. 18. Intended initial grasp.

A frictionless enveloping grasp must satisfy the equilibrium relationships

$$\mathbf{W}_n \, \mathbf{c}_n = -\mathbf{g}_{ext} \tag{1}$$

$$\mathbf{c}_n \geq 0, \tag{2}$$

for any external wrench acting on the object (recall that the subscript n identifies the normal components of the contact forces). Equivalently, the nonnegative column span of $\mathbf{W}_n$ must be equal to the space of possible external wrenches (for the two-dimensional problem, $\mathbf{g}_{ext} \in R^3$, where R^3 represents Euclidean three-space). Another way to think of envelopment is that if the joints are locked, then the object cannot move. That is, the object is completely restrained by the form or surface of the hand. This constraint condition is expressed by substituting 0 for $\dot{\theta}$ in inequality (47),

$$\mathbf{W}_n^T \, \dot{\mathbf{q}}_{ob} \geq 0 \tag{68}$$

and requiring that only the trivial solution exist (i.e., $\dot{\mathbf{q}}_{ob} \equiv 0$).

A second type of stable grasp is called a force closure grasp. It still satisfies relationships (1) and (2), but not for all possible external wrenches. For force closure, the nonnegative column span of $\mathbf{W}_n$ defines a convex cone C^+ (Goodman and Tucker 1956) that is a subset of the space of possible external wrenches. If the negative of the external wrench lies within C^+, then the grasp exhibits force closure. Therefore stability depends on the external wrench or force, hence the name "force closure." Figure 17(B) shows a force closure grasp. If gravity were acting up the page instead of down, the object would fall toward the palm.

Assuming our goal is to perform safe pick-and-place operations, each object must be manipulated away from its support surface and into an enveloping grasp. To achieve this goal, planning is broken into two phases: the *pre-liftoff* phase and the *lifting* phase.

3. Pre-Liftoff Phase

The objective of the pre-liftoff phase is to find a realizable initial grasp that guarantees that the object can be manipulated away from the support while moving closer to the palm. The simplest way to achieve this objective is to choose a grasp in the translation region. Squeezing then causes the object to translate upward, breaking all contact with the support (Fig. 18). All possible initial grasps of this type can be found using the following procedure:

1. Designate one finger to lie along an edge of the polygon.
2. Compute the translation region T.
3. Solve for the joint angles to contact the object in T with the other finger.
4. Check for geometric interference.
5. If T is empty or step 3 has no solution or interference is detected, reject the grasp; otherwise accept the grasp as feasible.
6. Return to step 1 until all combinations of finger and edge have been considered.

When choosing an initial grasp, preference should be given to those for which the second contact point is near the center of a large translation region, because those grasps will be least sensitive to position errors. For example, consider the intended initial grasp shown in Figure 18. Position errors could cause any or all of

Fig. 19. Grasp with self-correcting type 3 error.

the following scenarios:

1. Error in vertical position of finger 1, δy: $\mathbf{q}_{1g}$ moves up or down.
2. Error in the angle of finger 2, $\delta\psi_2$: the normal of contact 2 is altered.
3. Error in the angle of finger 1, $\delta\psi_1$: contact 1 or contact 5 is not achieved.

Errors of types 1 and 2 do not deleteriously affect the nature of liftoff of the object as long as the vertical error δy and the angular error $\delta\psi_2$ adhere to the following inequality:

$$\delta y - \rho_{cg}\frac{\delta\psi_2}{\cos\psi_2} < l_{2g}, \tag{69}$$

where ρ_{cg} is the distance from the center of gravity of the object to the second contact point, and l_{2g} is the distance between the points $\mathbf{q}_{1g}$ and $\mathbf{q}_{2g}$. Inequality (69) is valid if $\delta\psi_2$ is small.[5] Violation of inequality (69) implies that the second contact normal $\hat{\mathbf{n}}_2$ passes below the translation window, placing the contact in region $B4$. Thus the object will tip maintaining the third contact, defeating our goal. The third type of error causes the translation window to shrink to a point, either $\mathbf{q}_{1g}$ or $\mathbf{q}_{5g}$. Therefore $\hat{\mathbf{n}}_2$ passes either above or below the translation window, respectively. In the former case, the angle of finger 1 is less than commanded. Since the translation window becomes the point $\mathbf{q}_{1g}$, $\hat{\mathbf{n}}_2$ passes above it, so the grasp is in region $B3$. Upon squeezing, the object will rotate clockwise, aligning its edge with finger 1. This alignment opens the translation window and changes the nature of the grasp back to what was originally intended. Continued squeezing causes the object to translate up finger 1. In the latter case, the angle of finger 1 is too large, causing the translation window to become the point $\mathbf{q}_{5g}$, and the second contact to be in region $B4$. Again, squeezing causes an aligning rotation of the polygon followed by translation up the finger as planned. Figure 19(A) illustrates an initial grasp exhibiting the third type of error. As squeezing commences, the polygon's rightmost edge aligns with the edge of the finger [Fig. 19(B)]. Continued squeezing causes the object to translate up the finger [Fig. 19(C)].

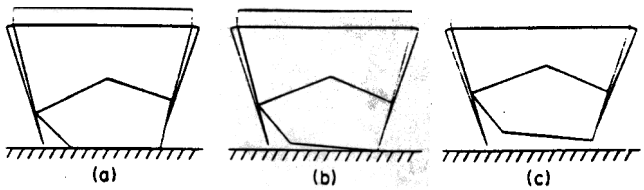

5. A similar expression applies if the contact is on an edge of the object rather than a vertex.

3.2. Lifting Phase

The lifting phase begins when the object no longer contacts the support. For this to occur, the object must be in a force closure grasp in the hand. No contact may remain on the support.

The goal of the lifting phase is to manipulate the object into an enveloping grasp. In doing so, the object may either be stable through force closure or unstable. Instability is undesirable, because it results in the object's falling. Even though an unstable object will eventually come to rest in a stable configuration, the final configuration cannot be predicted by our quasi-static technique. Therefore it is imperative that an enveloping grasp be gained without ever losing force closure.

Assume that the initial grasp has been chosen in the translation region. As lifting begins, the object contacts the hand at two points on one finger and at one point on the other. Since force closure requires three contacts, all must be maintained until a fourth contact is achieved. If the object is enveloped (i.e., the grasp has form closure), then the grasp is complete, and the lifting phase ends. If not, one contact must break as manipulation continues. Thus during the lifting phase, the object must translate relative to one of the fingers (assuming flat fingers) until the object contacts the palm. Once the palm has been contacted, translation is possible only if one finger loses contact with the object. In an enveloping grasp, both fingers and the palm must contact the object. Therefore we prefer to manipulate the object maintaining contact with both

Fig. 20. Convex cone C^+ projected onto the lifting phase plane.

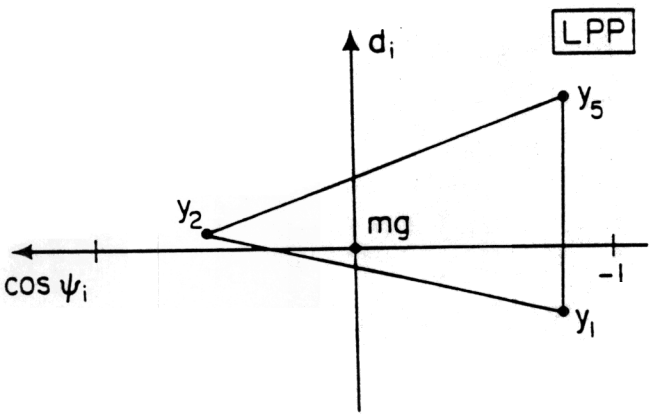

Fig. 21. Trajectory of $\mathbf{y}_2$.

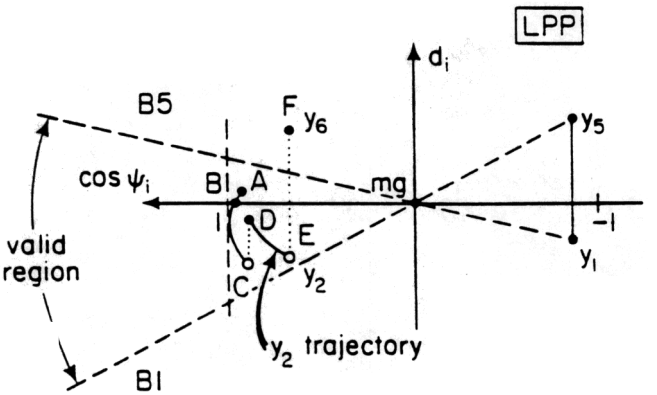

fingers. However, we analyze one planning strategy that allows contact to be lost with one finger as the object slides on the other.

A force closure grasp is one for which the negative of the gravitational wrench acting on the object is within the convex cone C^+ defined by equations (1) and (2). Examination of the equilibrium relationships (1) and (2) reveals how to manipulate a force closure grasp to achieve envelopment. Denote by $\mathbf{y}_i$, the ith column of $\mathbf{W}_n$

$$\mathbf{y}_i = \begin{matrix} \cos \psi_i \\ \sin \psi_i \\ d_i \end{matrix} \tag{70}$$

where recall ψ_i is the angle of the ith contact normal, and d_i is the moment of that contact normal measured with respect to the summing point $\mathbf{q}$. Choosing $\mathbf{q}$ to be the center of gravity of the object, the gravity moment is zero during manipulation. Thus the convex cone can be projected onto the *lifting phase plane* (LPP) formed by the $\cos \psi_i$ and d_i axes. In this plane, the cone becomes the LPP triangle, the gravity wrench maps to the origin, and two contacts on a flat link map to points on a vertical line separated by the distance that separates the contacts on the link (Fig. 20). The necessary and sufficient conditions for a grasp to have force closure are that (1) the LPP triangle enclose the origin and (2) the sine of the difference of the contact angles on the two fingers be greater than zero:

$$\sin (\psi_1 - \psi_2) > 0. \tag{19}$$

We desire to squeeze the object until it contacts the palm. However, while squeezing we must make sure that the LPP triangle always contains the origin and inequality (19) is never violated. If the initial grasp is in the translation region, then initially both of the conditions are satisfied. As the fingers are squeezed together, the quantity $\psi_1 - \psi_2$ may only decrease (if the singly contacted finger contacts a vertex of the object) or remain constant (if the singly contacted finger contacts an edge of the object). Because the palm eventually prevents squeezing from continuing, the quantity is bounded from below by zero. At the state of manipulation, the angular difference between the contact normals, $\psi_1 - \psi_2$, is in the interval bounded by zero and pi. During squeezing, the difference reduces but remains in the interval. Because the sine function is positive in that interval, the second condition is guaranteed to be satisfied thrqughout the entire manipulation.

The condition that the LPP triangle always contain the origin must be checked by considering the trajectories of the triangle's vertices. Their positions are affected by three variables, the two joint angles, θ_1 and θ_2, and the angle of the palm θ_p (see Fig. 18). Consider the hypothetical trajectory shown in Figure 21. Because the object will translate up finger 1, finger 2 (called the *pusher*), is rotated counterclockwise while finger 1 is held stationary. As the pusher rotates, vertices $\mathbf{y}_1$ and $\mathbf{y}_5$ of the LPP triangle remain fixed while vertex $\mathbf{y}_2$ follows a path qualitatively like the one shown beginning at point A. At the point C, $\mathbf{y}_2$ jumps to D. The discontinuity is caused by the edge of the second finger contacting the kth vertex $\mathbf{v}_k$ of the object

Fig. 22. Failed pusher strategy.

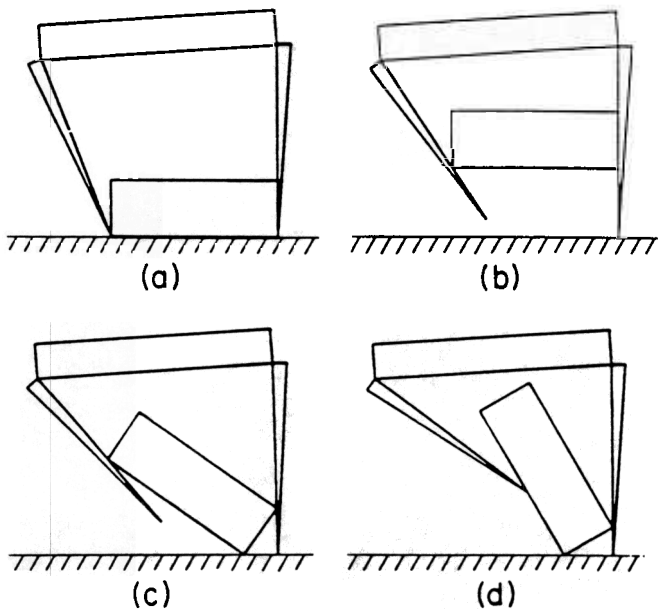

Fig. 23. LPP trajectories for hand rolling strategy.

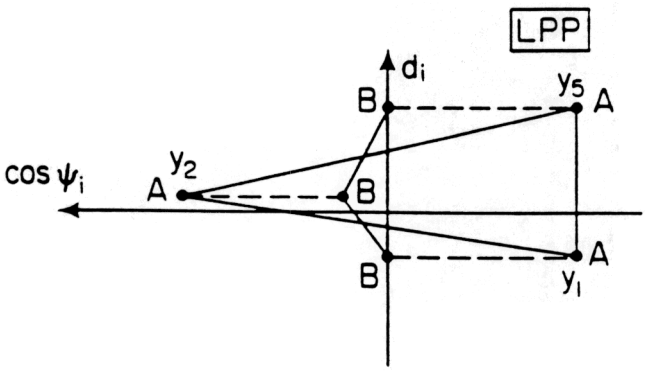

(see Fig. 18). At the instant the discontinuity occurs, there are four contacts, but only three can be maintained as the fingers continue to squeeze. Since D is within the valid region for the second vertex, the new contact remains, and the previous contact on that finger breaks. At the point E, the trajectory jumps outside the valid region to the point F. If the new contact were to remain (as it did at D), the interior of the LPP triangle would exclude the origin, and the object would become unstable. However, the trajectory jumped into the region labeled $B5$. This means that the fifth contact point (which is on finger 1) will break. The new LPP triangle has vertices labeled y_1, y_2, and y_6. Since the new vertices contain the origin, the grasp is still stable, but now the object will slide up the second finger rather than the first. Continuing squeezing, the first finger now acts as the pusher, rotating clockwise, and the second finger is held fixed. This strategy of using one finger as a pusher and holding the other finger fixed is called the *pusher strategy.*

An interesting property of the LPP trajectory is that if a vertex moves out of the valid region in a continuous manner, the object becomes unstable, because a contact point is lost without gaining a new one. However, if the vertex jumps outside the valid region (as at F), the object remains stable, and the finger on which the object translates switches. Any motion of the trajectory (continuous or not) within the valid region represents stable translation of the object without switching pushers.

If direct application of the pusher strategy fails (Fig. 22), one could try the *roll strategy* during which the finger angles are fixed as the palm is rotated (and translated upward if necessary). If the hand can be rotated far enough without losing force closure, the object will slide down the finger until it touches the palm. Afterward, the fingers may be closed around the object creating an enveloping grasp. Figure 23 shows the trajectories of the vertices of the LPP triangle corresponding to a clockwise rotation of the hand shown in Figure 18. As the hand rotates, the object does not move relative to it, and therefore the moment arms, d_i; $i \in \{1, 2, 5\}$, of the contacts do not change. The result is that the corners of the LPP triangle can move only horizontally, and since the normals of contacts 1 and 5 have the same direction, y_1 and y_5 move at a common rate. At B the right finger becomes horizontal. After slightly more rotation, the second contact breaks, and the object slides toward the palm. Closing the fingers around the object achieves the enveloping grasp.

We would like to know what conditions guarantee the success of the roll strategy. A condition of necessity is that d_1 and d_5 have opposite signs. If they have the same sign, the object could not be stable when sliding down the finger, because the gravity force would not pass between the two supporting contacts. Given that necessity is met, a sufficient condition is that d_2 equal zero. The validity of this condition can be argued for

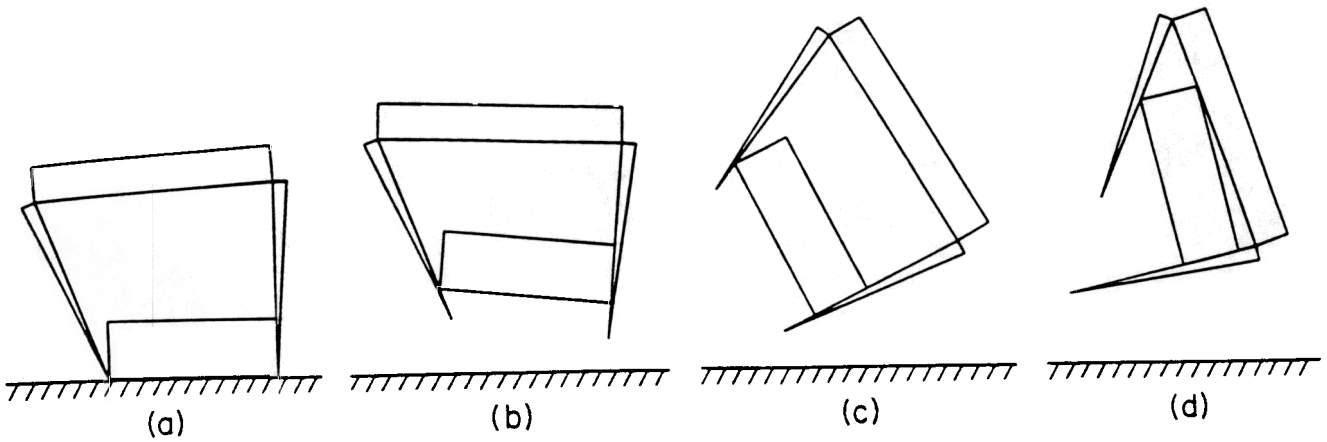

as follows. Since the grasp satisfies inequality (19), $\mathbf{y}_2$ is always on the left side of the lifting phase plane. As the hand rotates clockwise, $\mathbf{y}_1$ and $\mathbf{y}_5$ move toward the left. Until the right finger becomes horizontal, $\mathbf{y}_1$ and $\mathbf{y}_5$ are on the right side of the LPP. Therefore the LPP triangle always contains the origin. As the right finger passes through horizontal, $\mathbf{y}_1$ and $\mathbf{y}_5$ cross the d_i axis, causing the second contact to break as the object slides toward the palm on finger 1.

The pusher and roll strategies can be combined as illustrated in Figure 24. If possible, the pusher strategy should be used to cause vertex $\mathbf{y}_2$ to move to the cos ψ_i axis (see point B in Figure 21). After this, the roll strategy can be used to widen the valid region in the LPP so that manipulation can be safely completed. This is easily done in the manipulation sequence shown in Figure 24, because d_1 and d_5 have opposite signs.

If friction is present, the same strategies are valid, but inequality (40)

$$\sin(\phi_{15} - \phi_2) > 0 \tag{40}$$

must be satisfied rather than inequality (19), and each edge, $\mathbf{y}_i$, of the convex cone must be replaced with $\tilde{\mathbf{y}}_i$, the appropriate edge of the friction cone for each contact:

$$\tilde{\mathbf{y}}_i = \begin{bmatrix} \cos(\psi_i + \alpha) \\ \sin(\psi_i + \alpha) \\ \tilde{d}_i \end{bmatrix}; \quad i \in (1, 5) \qquad \tilde{\mathbf{y}}_2 = \begin{bmatrix} \cos(\psi_2 \pm \alpha) \\ \sin(\psi_2 \pm \alpha) \\ \tilde{d}_2 \end{bmatrix} \tag{79}$$

where $\tilde{d}_i$ is the moment arm of the ith contact force and α is the friction angle. The sign of α in the expression for $\tilde{\mathbf{y}}_2$ is dependent on the relative velocity of the second contact point. Since it would be useful to control the sign of α, it would be preferable that the second finger have more than one link.

4. Conclusion

Manipulation with articulated hands is usually carried out under force control to prevent slipping at the contacts. Dissallowing slipping unnecessarily limits the dexterous capability of a hand and cannot be done in the absence of friction. We have addressed the problem of achieving an enveloping grasp in the plane based on sliding contacts. Our solution was based on the frictionless case but extended where possible to include Coulomb friction. Planning was broken into two phases, the *pre-liftoff phase* and the *lifting phase*. The goal of the pre-liftoff phase was to manipulate the object to cause it to lose contact with its support. This led us to define and analyze the *liftability* of planar objects. Given the contact configuration of one finger, the *liftability regions* of the object could be determined and used to plan the placement of the other finger to complete the initial grasp. It was determined that initial grasps in the *translation region* of the object should be used, because they achieve the goal of

the pre-liftoff phase most directly and are insensitive to position errors. For the lifting phase, planning was done geometrically in the *lifting phase plane*, providing a simple method to monitor grasp stability and to predict which contacts were gained and lost as the grasp evolved. Manipulation trajectories generated by our planning technique can be executed under position control; servo control of contact forces is unnecessary even when friction is active. However, a modicum of contact force sensing or monitoring would be useful to abort execution of manipulation plans if unexpected jamming is detected.

Even though our analysis in section 3 was two dimensional, the planning methods can be applied to three-dimensional objects that can be modeled as generalized cylinders by planning manipulation using the appropriate cross sections of the cylinders. In the event that such modeling is inappropriate, the *forward object motion problem* that we have formulated can be used incrementally to plan manipulation trajectories in three dimensions. By-products of planning using the forward object motion problem are the predicted time histories of the contact forces. These histories could be used to determine whether the planned manipulation would be likely to damage the proposed (fragile) work piece.

7. Appendix

Here we show how the liftability regions of two two-point initial grasps can be combined to form the liftability regions of one three-point initial grasp.

7.1. The Sliding Region, S

The sliding region S for an object is independent of the number and positions of finger contacts; it depends only on the geometry of the object [see inequality (22)]. Therefore we immediately write the following equation:

$$S = S_1 = S_5. \tag{35}$$

7.2. The Region S'

The other relevant liftability regions are J, $B3$, $B4$, T, J_1, $B3_1$, $B4_1$, T_1, J_5, $B3_5$, $B4_5$, and T_5, where the non-subscripted regions are a result of the three-point initial grasp, and the subscript i; $i \in \{1, 5\}$ implies a two-point grasp using contacts 2 and i. The liftability regions of the two two-point initial grasps must satisfy the following equations:

$$J_1 \cup B3_1 \cup B4_1 \cup T_1 = S'$$

$$J_5 \cup B3_5 \cup B4_5 \cup T_5 = S'$$

We begin our derivation of equations (36)–(39) with the following true statement:

$$S' \cap S' = S'.$$

Substituting equations (A1) and (A2) into (A3) and expanding gives

$$\begin{aligned}&(J_1 \cap J_5) \cup (J_1 \cap B3_5) \cup (J_1 \cap B4_5) \cup (J_1 \cap T_5)\\ &\cup (B3_1 \cap J_5) \cup (B3_1 \cap B3_5) \cup (B3_1 \cap B4_5) \cup (B3_1 \cap T_5)\\ &\cup (B4_1 \cap J_5) \cup (B4_1 \cap B3_5) \cup (B4_1 \cap B4_5) \cup (B4_1 \cap T_5)\\ &\cup (T_1 \cap J_5) \cup (T_1 \cap B3_5) \cup (T_1 \cap B4_5) \cup (T_1 \cap T_5) = S'.\end{aligned} \tag{A4}$$

Because the liftability regions for each two-point initial grasp are mutually exclusive, the 16 sets formed by intersection in equation (A4) are mutually exclusive.

Any set that is formed by intersection with J_1 or J_5 belongs to J. This statement is motivated physically by the fact that for a two-point initial grasp in the jamming region, the object can only be further constrained by adding another contact point. Noting that the top row and the leftmost column of the left side of equation (A4) are equivalent to J_1 and J_5, respectively, we write:

$$J \supset J_1 \cup J_5. \tag{A5}$$

Equation (A5) accounts for seven of the sets in equation (A4).

The nature of liftoff for the remaining nine sets can be deduced by considering Figure A1 using the following facts:

Fig. A1. Formation of the region $B3_1 \cap B3_5$.

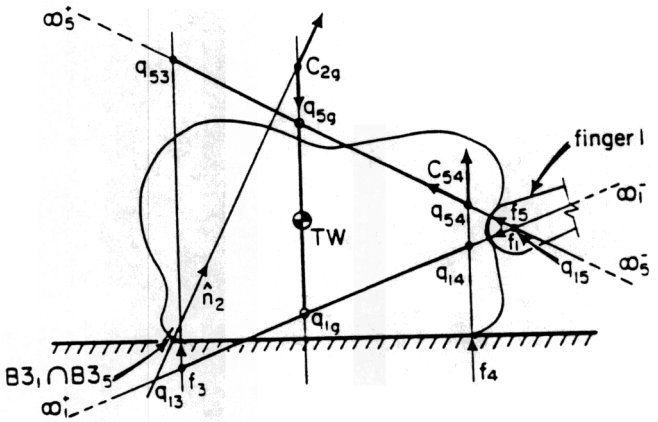

1. A stable grasp must have three contact points during manipulation (more contacts cause static indeterminacy and interference; fewer lead to grasp instability).
2. The positive or negative cones of a stable grasp must "see each other" (Nguyen 1986) where the positive force cone of $\mathbf{f}_4$ and $\mathbf{f}_5$ is labeled in Figure A1 as C_{54}.
3. The positive or negative force cone is the set of points defined respectively by a positive or negative linear combination of the forces using their intersection as the cone's apex.
4. A pair of cones see each other or are mutually visible if each cone contains the other's apex.

Consider the set $B3_1 \cap B3_5$. Referring to Figure A1, a point in S' can only belong to both $B3_1$ and $B3_5$ in two ways: the contact normal $\hat{\mathbf{n}}_2$ passes upward through both open half lines $(\mathbf{a}_{5g}, \infty_5^+)$[6] and $(\mathbf{q}_{1g}, \infty_1^+)$ (as shown in Figure A1) or downward through both half lines $(\mathbf{q}_{14}, \infty_1^-)$ and $(\mathbf{q}_{54}, \infty_5^-)$. Let one force cone be C_{2g} as shown.[7] To determine the nature of liftoff, we must find a cone within sight of C_{2g} that can see C_{2g}. Only cones C_{14} and C_{54} satisfy this requirement. Since neither cone is constructed using the third contact force, that contact must break (i.e., the grasp must be in $B3$). Both cones include the fourth contact force so that contact is maintained. However, to maintain exactly three contacts during manipulation, either the first or fifth contact must also break. The one that will break is determined by considering the motions that will be made by the fingers. For example, if finger 1 remains fixed as finger 2 squeezes, then the first contact will break while the fifth contact is maintained. In this case the instantaneous center of rotation of the object is either the point $\mathbf{q}_{14}$ or $\mathbf{q}_{54}$. If we assume that the fifth contact breaks, this implies that the center of rotation is $\mathbf{q}_{14}$. Rotation counterclockwise about $\mathbf{q}_{14}$ causes interference at the third contact; clockwise rotation causes interference at the fifth contact. Thus the assumption that the fifth contact breaks is inconsistent with the instantaneous kinematics of the grasp. Therefore the first contact (and the third contact) must break, while the fifth contact (along with the second and fourth contacts) is maintained. This conclusion is validated by the fact that instantaneous clockwise rotation about $\mathbf{q}_{54}$ does not cause interference.

The result of the above arguments is that we may write:

$$B3 \supset B3_1 \cap B3_5$$

By a similar argument one can show that

$$B4 \supset B4_1 \cap B4_5$$

$$T \supset B3_1 \cap T_5$$

$$T \supset B4_5 \cap T_1$$

Also, because in S' the contact normals $\hat{\mathbf{n}}_2$ must have a horizontal component to the right, we note that it is impossible for any contact point to be in both sets $B4_1$ and $B3_5$:

$$B4_1 \cap B3_5 = \varnothing,$$

where $\varnothing$ represents the null set. For a contact point to be elements of both sets would require that the contact normal pass upward through $(\mathbf{q}_{1g}, \infty_1^-)$ or downward through $(\mathbf{q}_{13}, \infty_1^+)$ and upward through $(\mathbf{q}_{5g}, \infty_5^+)$ or

6. By ". . . upward through the half-line $(\mathbf{q}_{5g}, \infty_5^+)$ . . . ," we imply the satisfaction of $\sin(\psi_5 - \psi_2) > 0$. Similarly, "downward" implies satisfaction with the inequality reversed. To define upward and downward with respect to half lines along the line of the first contact force, substitute ψ_1 for ψ_5.

7. To make two cones requires four forces. They are the three contact forces and the gravity force.

Fig. A2. Partitioning of the region $B3_1 \cap B4_5$ *into regions* J_T *and* T.

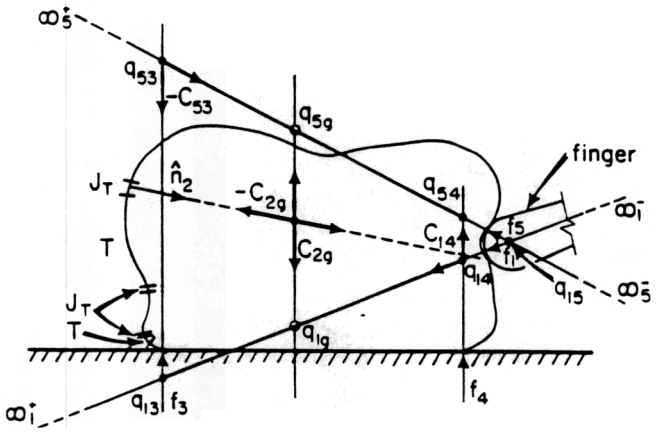

downward through $(\mathbf{q}_{54}, \infty_5^-)$, which is impossible. Similar arguments result in the following three equations:

$$B3_5 \cap T_1 = \varnothing \tag{A11}$$

$$B4_1 \cap T_5 = \varnothing \tag{A12}$$

$$T_1 \cap T_5 = \varnothing. \tag{A13}$$

The only set not accounted for is $B3_1 \cap B4_5$. All contact normals belonging to this set must pass through the translation window $(\mathbf{q}_{1g}\ \mathbf{q}_{5g})$. Consider the cone C_{2g} shown in Figure A2. If $\hat{\mathbf{n}}_2$ passes through $(\mathbf{q}_{5g}, \mathbf{q}_{15})$, then C_{15} and C_{2g} see each other (i.e., the grasp is in the translation region). If $\hat{\mathbf{n}}_2$ passes through $(\mathbf{q}_{14}, \mathbf{q}_{15})$,[8] then the only pairs of mutually visible cones are C_{2g}, C_{14} and $-C_{2g}$, $-C_{53}$. The corresponding instantaneous centers of rotation are the points $\mathbf{q}_{14}$ and $\mathbf{q}_{53}$, respectively. The first pair of cones implies that the third contact must break, which requires counterclockwise rotation about $\mathbf{q}_{14}$. This rotation causes interference at the fifth contact. The second pair of cones implies that the fourth contact must break, which requires clockwise rotation about $\mathbf{q}_{53}$. This rotation causes interference at the first contact. Therefore we conclude that motion is impossible. Thus

8. Note that contact normals that pass through TW and $(\mathbf{q}_{1g}, \mathbf{q}_{14}]$ have already been assigned to the jamming region by relationship (A5).

points in S' whose normals pass through the translation window TW and through $(\mathbf{q}_{14}, \mathbf{q}_{15})$ belong to J_T, which is a subset of J. For the case of $\mathbf{q}_{15}$ on the left of the translation region, the procedure for defining T and J_T is identical, except the segments $(\mathbf{q}_{5g}, \mathbf{q}_{15})$ and $(\mathbf{q}_{14}, \mathbf{q}_{15})$ must be replaced by $(\mathbf{q}_{15}, \mathbf{q}_{1g})$ and $(\mathbf{q}_{15}, \mathbf{q}_{53})$, respectively. The set $(B3_1 \cap B4_5)$ can now be written as the union of two mutually exclusive sets:

$$B3_1 \cap B4_5 = J_T \cup (J_T' \cap B3_5 \cap B4_1), \tag{A14}$$

where the second term on the right side represents the portion of the set $(B3_1 \cap B4_5)$ that is in the translation region. Also note that for a grasp in the translation region with finger 1 fixed, $\mathbf{q}_{15}$ is the instantaneous center of rotation and must lie to the left or right of the line of action of $\mathbf{f}_3$ or $\mathbf{f}_4$, respectively. If $\mathbf{q}_{15}$ lies between $\mathbf{f}_3$ and $\mathbf{f}_4$, rotation counterclockwise or clockwise causes interference at the third and fourth contacts, respectively, a contradiction that both contacts three and four break simultaneously.

The nature of liftoff for all 16 sets of S' have been determined and are now combined to yield the liftability regions for the three-point initial grasp:

$$B3 = B3_1 \cap B3_5 \tag{36}$$

$$B4 = B4_1 \cap B4_5 \tag{37}$$

$$J = J_1 \cup J_5 \cup J_T \tag{38}$$

$$T = (B3_1 \cap B4_5 \cap J_T') \cup (B3_1 \cap T_5) \cup (B4_5 \cap T_1). \tag{39}$$

Q.E.D.

5. Acknowledgments

We would like to extend our thanks to Dr. J. M. Abel and Dr. M. C. Peshkin for their suggestions. This research was performed at the University of Pennsylvania and the University of Wollongong and was supported in part by the following grants: IBM 6-28270. ARO DAA6-29—84-k-0061, AfOSR 82-NM-299, NSF ECS 8411879, NSF MCS-8219196-CER, NSF

MCS 82-07294, AVRO DAAB07-84-K-F077, and NIH 1-RO1-HL-29985-01. Any opinions, findings, conclusions, or recommendations expressed in this publication are those of the authors and do not necessarily reflect the views of the granting agencies.

6. References

Asada, H., and By, A. 1984 (August, Kyoto, Japan). Kinematic analysis and design for automatic workpart fixturing in flexible assembly. *Proc. Second International Symposium on Robotics Research.* Cambridge: MIT Press, pp. 50–57.

Beveridge, G. S. G., and Schechter, R. S., 1970. *Optimization: Theory and Practice.* New York: McGraw-Hill.

Brock, D. L. 1988. Enhancing the dexterity of a robot hand using controlled slip. M.S. thesis, Department of Mechanical Engineering, Massachusetts Institute of Technology.

Brooks, R. A. 1983. Planning collision-free motions for pick-and-place operations. *Int. J. Robot. Res.* 2(4):19–44.

Brost, R. C. 1985. Planning robot grasping motions in the presence of uncertainty. CMU-RI-85-12. Pittsburgh: Carnegie-Mellon University, Department of Computer Science.

Cutkosky, M. R. 1985. *Robotic Grasping and Fine Manipulation.* Boston: Kluwer Academic Publishers.

Erdmann, M. A., and Mason, M. T. 1986 (April, San Francisco). An exploration of sensorless manipulation. *Proc. International Conference on Robotics and Automation.* New York: IEEE, pp. 1569–1574.

Fearing, R. S. 1986. Simplified grasping and manipulation with dexterous robot hands. *IEEE J. Robot. Automat.* 2(4):188–195.

Fearing, R. S. 1987 (March–April, Raleigh, North Carolina). Some experiments with tactile sensing during grasping. *Proc. International Conference on Robotics and Automation.* New York: IEEE, pp. 1637–1643.

Goldman, A., and Tucker, A., 1956. Polyhedral convex cones. In Kuhn, H., and Tucker, H. (eds.): *Linear Inequalities and Related Systems.* Princeton, N.J.: Princeton University Press, pp. 19–40.

Hanafusa, H., and Asada, H. 1982. Stable prehension by a robot hand with elastic fingers. In Brady, M., et al. (eds.): *Robot Motion.* Cambridge: MIT Press, pp. 337–359.

Holzmann, W., and McCarthy, J. M. 1985 (March, St. Louis). Computing the friction forces associated with a three-fingered grip. *Proc. International Conference on Robotics and Automation.* New York: IEEE, pp. 594–600.

Jameson, J. W. 1985. Analytic techniques for automated grasp. Ph.D. dissertation, Department of Mechanical Engineering, Stanford University.

Ji, Z. 1987. Dexterous hands: Optimizing grasp by design and planning. Ph.D. dissertation, Department of Mechanical Engineering, Stanford University.

Kerr, J. R. 1984. An analysis of multi-fingered hands. Ph.D. dissertation, Department of Mechanical Engineering, Stanford University.

Kobayashi, H. 1984 (August, Kyoto, Japan). On the articulated hands. *Proc. Second International Symposium on Robotics Research.* Cambridge: MIT Press, pp. 128–135.

Lakshminarayana, K. 1978. The mechanics of form closure. Report 78-DET-32. New York: ASME.

Lanczos, C. 1986. *The Variational Principles of Mechanics.* Toronto: University of Toronto Press.

Laugier, C., and Pertin, J. 1983. Automatic grasping: A case study in accessibility analysis. Research report 342. Toulouse, France: LIFIA.

Li, Z., and Sastry, S. 1987 (March–April, Raleigh). Task oriented optimal grasping by multi-fingered robot hands. *Proc. International Conference on Robotics and Automation.* New York: IEEE, pp. 389–394.

Mason, M. T. 1979. Compliance and force control for computer controlled manipulators. M.S. thesis, Department of Computer Science, Massachusetts Institute of Technology.

Mason, M. T., and Salisbury, J. K. 1985. *Robot Hands and the Mechanics of Manipulation.* Cambridge: MIT Press.

Nguyen, V-D. 1986. The synthesis of stable force-closure grasps. M.S. thesis, Department of Electrical Engineering and Computer Science, Massachusetts Institute of Technology.

Ohwovoriole, M. S. 1980. An extension of screw theory and its application to the automation of industrial assemblies. Ph.D. dissertation, Department of Mechanical Engineering, Stanford University.

Okada, T. 1982. Computer control of multijointed finger system for precise object handling. *IEEE Trans. Sys. Man Cybernet.* 12(3):289–298.

Paul, R. P. 1972. Modeling, trajectory calculation and servoing of a computer controlled arm. AIM-177. Stanford University, Palo Alto: Stanford Artificial Intelligence Laboratory.

Peshkin, M. A., and Sanderson, A. C. 1989. Minimization of energy is quasistatic manipulation. *IEEE Trans. Robot. Automat.* 5(1):53–60.

Peshkin, M. A., and Sanderson, A. C. 1988. The motion of a pushed, sliding workpiece. *IEEE J. Robot. Automat.* 4(6):569–598.

Salisbury, J. K. 1982. Kinematic and force analysis of articulated hands. Ph.D. dissertation, Department of Mechanical Engineering, Stanford University.

Trinkle, J. C. 1985. Frictionless grasping. MS-CIS-85-46, GRASP Lab 52. Philadelphia: University of Pennsylvania, Department of Computer and Information Science.

Trinkle, J. C. 1987. The mechanics and planning of enveloping grasps. Ph.D. dissertation, Department of Systems Engineering, University of Pennsylvania.

Trinkle, J. C. 1988. An investigation of frictionless, enveloping grasping in the plane. *Int. J. Robot. Res.* 7(3):33–51.

Whitney, D. E. 1982. Quasi-static assembly of compliantly supported rigid parts. *J. Dyn. Sys. Meas. Control* 104:65–77.

Wolter, J. D., Volz, R. A., and Woo, A. C. 1984. Automatic generation of gripping positions. Technical report. Ann Arbor: University of Michigan, Department of Mechanical Engineering.